# Strain variations in concrete subjected to cyclic freezing and thawing

凍結融解下におけるコンクリートのひずみの変化

**Shashank Bishnoi**

A Thesis Submitted to University of Tokyo
In partial fulfillment of the requirements for
The Degree of Master of Engineering

| Signature | Date | Seal |
|---|---|---|
| Advisor: | | |
| Co-Advisor: | | |

Supervisor
**Professor Uomoto Taketo**

Department of Civil Engineering
University of Tokyo
Tokyo, Japan
September 2004

# ACKNOWLEDGEMENT

The few names written on the cover of this thesis cannot do justice to everyone whose efforts went into making the work possible. As I'm about to finish writing this volume, I look back and can't imagine having to do even half of all that went into it all by myself. I would thus like to take this opportunity to thank everyone who helped me, not only in the research work, but also otherwise.

Firstly I would like to thank Prof. Uomoto for accepting me in his laboratory and providing me invaluable guidance throughout my stay of around two years here. Next I would thank Prof. Kishi and Prof. Kato who spent countless number of hours out of their busy schedules discussing my research and encouraging me. I would also like to thank Prof. Ishida for discussing my research with me and pointing out the weak points helping me improve my work. Perhaps the one name I cannot miss writing here is that of Prof. Misra of IIT Kanpur, India, who helped me form my first mental image of concrete and has continuously been guiding and motivating me for the last four years.

I would then like to thank Mr. Hoshino who always had useful bits of experience from his long years in concrete to share and was always ready to lend me a helping hand during my experiments. Talking of experience, I thank Mr. Nishimura for always knowing that I'm about to land into trouble and being at that exact place at the exact time getting rid of my trouble within a moment! As a matter of fact every one in the Uomoto-Kishi-Kato Laboratory has been more than supportive and has helped me in my research and made my life more enjoyable in Japan. I should specially thank Mr. Kanada, who helped me settle down in Japan and get used to the Japanese way of life and still finds time to help me out from his busy research schedule. I should also thank Mrs. Ochi and Mrs. Yoshimoto, who added much needed the touch of home to my life in Japan.

Throughout my two years in Japan, though far away in India, my family has continuously supported and encouraged me to keep working. My stay in Japan wouldn't have been possible without their encouragement. I also thank my fiancée for teaching me to keep faith in myself and spending countless hours each day giving me the drive to keep working.

Last, but not the least, I should thank the Japanese Ministry of Education, Culture, Sports, Science and Technology for selecting me for the generous Monbu-kagaku-sho scholarship which made it possible for me to join the University of Tokyo and to live in Japan.

# ABSTRACT

Freeze-thaw deterioration of concrete poses a major problem for infrastructure in countries experiencing sub-zero temperatures and various efforts since the introduction of air-entraining admixtures into construction since 1930 have led to the present state-of-the-knowledge. This research is an attempt to further understand the process of freeze-thaw deterioration by measuring strain and temperature variations within concrete using accelerated tests. Specimens of different sizes with embedded strain gauges were prepared using various mix-proportions and were subjected to accelerated cyclic freeze-thaw conditions immersed in water and strain and temperature variations inside the specimens were measured at regular short intervals. The effect of presence of excess water outside specimens was also studied using similar specimens in the absence of water outside and alternating conditions.

It was observed that damage is insignificant in the absence of water and high rates of damage were observed in cases where water was available on the surface of the specimens. Air-entrained specimens showed much lower levels of deterioration even under aggressive conditions.

Variation of strain with temperature and with the progress of cycles has been presented in this study. Residual strains and the strain-temperature behavior were found to change due to deterioration and have been proposed to be used to evaluate extent of deterioration of concrete. Effects of various factors on this variation have also been discussed.

Further, the results obtained from the study have been used to take a closer look at the process of freeze-thaw deterioration. Changes in apparent thermal expansion coefficient were observed due to wetting and drying of gel pores due to ice-accretion. It has been shown that measurement of variation of this parameter can give an insight to the processes in action during cyclic freeze-thaw deterioration.

It is thus shown that strain is an important parameter for structures under freeze-thaw conditions and can be used to obtain quantitative assessment of damage in concrete subjected to freeze-thaw deterioration and can also afford a view of the microscopic phenomenon in progress during freeze-thaw deterioration.

# CONTENTS

**Acknowledgement** (i)

**Abstract** (ii)

**Contents** (iii)

**List of Tables** (vii)

**List of Figures** (viii)

**Chapter 1: Introduction** **1**

1.1 Objectives 2

1.2 Research Significance 3

**Chapter 2: Cyclic Freeze-Thaw Deterioration: A Literature Review** **5**

2.1 Background 5

2.2 Mechanism of Freeze-Thaw Deterioration 6

2.3 Major Factors Affecting Deterioration 8

2.3.1 Water/Cement Ratio 9

2.3.2 Air Entrainment 9

2.3.3 Aggregates 9

2.3.4 Degree of Saturation 10

2.3.5 Curing 10

2.3.6 Freezing Rate 10

2.4 Prevention of Freeze-Thaw Deterioration 11

2.5 Strains during Freezing and Thawing 11

2.5.1 Water at Sub-Zero Temperatures 11

2.5.2 Previous Studies on Strain Variations 14
2.6 Pore-Structure of Concrete and Drying Shrinkage 16

**Chapter 3: Experiments: Procedures, Conditions and Brief Overview of Results 18**
3.1 Series 1: Temperatures and Strains 18
3.1.1 Specimen Specifications 18
3.1.1.1 Materials Used 18
3.1.1.2 Mix Design 20
3.1.1.3 Specimens: Design and Coding 20
3.1.1.4 Curing and Pre-Test Conditions 22
3.1.2 Freeze-Thaw Cycles: Test Conditions 22
3.1.2.1 Wet Cycles 22
3.1.2.2 Dry Cycles 24
3.1.3 Experimental Errors and Imperfections 24
3.1.3.1 Exposure Differences 24
3.1.3.2 Initial Water Gain 25
3.1.3.3 Drying During Measurements 25
3.1.3.4 Lost Data 26
3.1.4 Results 26
3.1.4.1 Weight Loss and Relative Dynamic Modulus 26
3.1.4.2 Temperature Variations 27
3.1.4.3 Strain Variations 30
3.2 Series 2: Effect of Water Ingress 32
3.2.1 Specimen Specifications 32
3.2.1.1 Mix Design 32
3.2.1.2 Specimens: Design and Coding 33
3.2.1.3 Curing and Pre-Test Conditions 33
3.2.2 Freeze-Thaw Cycles: Test Conditions 33
3.2.3 Experimental Errors and Imperfections 35
3.2.4 Results 37
3.2.4.1 Weight Loss and Relative Dynamic Modulus 37

3.2.4.2 Strain Variations 37
3.3 Other Series 38
3.3.1 Series 3: Longer Cycle Time 38
3.3.2 Series 4: Test for $\alpha_{app}$ over 0°C 39
3.3.3 Series 5: Specimens with Cracks 40

**Chapter 4: Discussion of Results 43**
4.1 Strain-Temperature Variation 43
4.1.1 Analytical Verification of Strains 43
4.1.1.1 Derivation of Strain Dependence on Temperature 44
4.1.1.2 Verification of Derived Relation 47
4.1.1.3 Comparison of Experimental and Calculated Strains 48
4.1.2 Anomalies in Strain-Temperature Curves 50
4.2 Residual Strains 52
4.2.1 Importance of Residual Strains 52
4.2.2 Slight Deteriorations 53
4.2.3 Severe Deteriorations 54
4.2.4 Effect of Degree of Saturation 55
4.3 Apparent Thermal Expansion Coefficient 58

**Chapter 5: The Process of Freeze-Thaw Deterioration 62**
5.1 Mechanisms Leading To Observations 62
5.1.1 Main Experimental Observations 62
5.1.2 Drying Shrinkage 63
5.1.3 Initial Cycles 63
5.1.4 Progressive Wetting of Specimens 64
5.1.5 Dry Specimens 65
5.1.6 Slow Temperature Rate 66
5.1.7 Progress of Deterioration 67
5.1.8 Possible Reduction of $\alpha_{app}$ to a Constant Value 69
5.1.9 Differences during Freezing and Thawing 69

5.1.10 Effect of Size of Specimen 70
5.1.11 Effect of Air-Entrainment 71
5.2 Process of Freeze-Thaw Deterioration 72
5.3 Substantiations of Progressive Ingress 73
5.3.1 Dilatations around 0°C 73
5.3.2 Severe Growth of Cracks in Pre-Cracked Specimens 74

**Chapter 6: Monitoring Freeze-Thaw Deterioration and Vulnerability 76**
6.1 Strain-Temperature Trend 76
6.2 Residual Strains 77
6.2.1 Uniform Moisture Conditions 77
6.2.2 Degree of Saturation 77
6.2.3 Freezing Expansions 78
6.2.4 Varying External Conditions 78
6.3 Apparent Thermal Expansion Coefficient 78
6.4 Suggested Further Research 79

**Chapter 7: Conclusions 80**

**References 82**

**Attachment: Compact disk containing experimental data in Microsoft Excel format.**

# LIST OF TABLES

Table 3.1: Composition of cement 19
Table 3.2: Properties of cement 19
Table 3.3: Unit (1 $m^3$) composition of concrete in Series 1 20
Table 3.4: Details of specimens in Series 1 21
Table 3.5: Weight loss (WL) and relative dynamic modulus (RDM) 26
Table 3.6: Unit (1 $m^3$) composition of concrete in Series 2 32
Table 3.7: Details of specimens in Series 2 33
Table 3.8: Specimen states for B type exposure condition 35
Table 3.9: Details of specimens in Series 5 40

# LIST OF FIGURES

Fig. 2.1: Air-void spacing vs. water-cement ratio for a durable mix 8
Fig. 2.2: Densities of ice and super-cooled water at sub-zero temperatures and cubic thermal expansion coefficient of ice 13
Fig. 2.3: Variation of melting point of ice with pressure 13
Fig. 2.4: Thermal properties of ice at sub-zero temperatures 13

Fig. 3.1: Particle size distribution of aggregates 19
Fig. 3.2: Placing of sensors 22
Fig. 3.3: Experimental setup 23
Fig. 3.4: Typical temperature variation in thermal exchange fluid in Series 1 23
Fig. 3.5: Difference in surface conditions for different specimen sizes 25
Fig. 3.6: Specimens 7-55-E-M, 10-55-E-M and 15-55-E-M at the end of all cycles 27
Fig. 3.7: Temperature variations at center of specimens during wet cycles 27
Fig. 3.8: Temperature variations in 10 cm specimens of different mix-proportions 28
Fig. 3.9: Temperature variations in 7 cm and 15 specimens of different mix-proportions 28
Fig. 3.10: Temperature variations at center of specimens during dry cycles 29
Fig. 3.11: Variation of strains against temperature during wet cycles 29
Fig. 3.12: Variation of strains against temperature during dry cycles 30
Fig. 3.13: Higher apparent thermal expansion coefficient below 0°C 31
Fig. 3.14: Typical temperature variation in thermal exchange fluid in Series 2 34
Fig. 3.15: Typical temperature variations at center of specimens in Series 2 35
Fig. 3.16: Weight loss in specimens in Series 2 36
Fig. 3.17: Reduction in Young's dynamic modulus in specimens in Series 2 36
Fig. 3.18: Specimens of Series 2 at the end of all Freeze-thaw cycles 37

Fig. 3.19: Temperature variations during 36-hour cycles 39
Fig. 3.20: Strain-Temperature variations during 36-hour cycles 39
Fig. 3.21: Crack in specimen before subjecting to freeze-thaw cycles 41
Fig. 3.22: Cracked specimens after freeze-thaw deterioration 41

Fig. 4.1: Simplifications in analytical thermal calculations 44
Fig. 4.2: Simplified modeling for strain calculations 46
Fig. 4.3: Comparison of calculated strains with FEM analysis 48
Fig. 4.4: Comparison of experimental results with calculated values 49
Fig. 4.5: Strain-temperature curves for un-entrained 7 cm specimens 50
Fig. 4.6: Strain-temperature curves for un-entrained 10 cm specimens 51
Fig. 4.7: Strain-temperature curves for air-entrained 10 cm specimens 51
Fig. 4.8: Residual strains in specimens in Series 1 54
Fig. 4.9: Residual strains for specimens in wet state throughout in Series 2 54
Fig. 4.10: Residual strains for specimens with dry cycles for Series 2 at -15°C 55
Fig. 4.11: Residual strains for Series 4 and 5 at -15°C 57
Fig. 4.12: Apparent thermal expansion coefficients during Series 1 58
Fig. 4.13: Apparent thermal expansion coefficients for specimens with severe deterioration 59
Fig. 4.14: Apparent thermal expansion coefficients for B-type conditions 59
Fig. 4.15: Apparent thermal expansion coefficients in Series 2 60
Fig. 4.16: Average apparent thermal expansion coefficients in Series 3 and 4 61

Fig. 5.1: The progress of freeze-thaw deterioration 68
Fig. 5.2: Effect of air-entrainment 72

# Chapter 1

# INTRODUCTION

Concrete, the most widely used construction material in the world, is full of unique peculiarities. The composite nature of concrete and its preparation using raw materials of natural origin with relatively lower levels of processing makes it vulnerable to various natural processes. It is ironic that water, one of the most important components of concrete, can be one of the major reasons of its deterioration. Still, it is difficult to imagine an urban settlement sans concrete. Throughout the 20th century, and now, into the 21st, researchers have been trying to understand the various processes taking place in the life span of concrete; however, every new discovery and theory proposed led to newer mysteries and bigger challenges in perfectly understanding the vital processes of concrete.

Through these years, the focus of attention has shifted through a wide spectrum of topics starting from basic properties such as strength and workability to more complex microscopic properties such as the process of hydration, with the recent years seeing a surge in research focusing on durability and life-span related problems. Ageing infrastructures and higher serviceability requirements have seen higher and still rising proportions of investments into repair and maintenance further highlighting the importance of considering durability aspects at the design stage itself.

Recent years have also seen the rise of various new monitoring and evaluation techniques. The tremendous size and often inaccessibility of structures can demand large amounts of man power and time in obtaining data that can help engineers make decisions regarding maintenance and repair and in determining

serviceability of the structure. This often increases the cost of repair and reduces the reliability of such studies emphasizing the need of simpler methods with increased objectivity requiring lesser man-power.

This study focuses on deterioration of concrete subjected to cyclic freezing and thawing. Freeze-thaw deterioration of concrete poses a major problem for infrastructure at locations experiencing sub-zero temperatures.

Research to tackle freeze-thaw related problems started in early 20th century with the introduction of air-entraining admixtures in 1930. The ensuing years witnessed a large amount of research evolving the viewpoint of the researchers and filling in gaps in the knowledge about the process and the accepted explanations for the phenomenon. However, this knowledge cannot still be termed complete. A variety of models and theories have been propounded over the years attempting to explain the process and predict concrete behavior under such conditions, but evaluation of freeze-thaw resistance of concrete is still primarily limited to accelerated laboratory tests evaluating the performance of small concrete specimens under simulated environmental conditions. The damage in these specimens is still periodically, rather than continuously measured, using measures like weight loss, dynamic elastic modulus, etc., which, though, relatively easy to measure in small specimens, are difficult to apply to larger structures.

## 1.1 OBJECTIVES

This study is an effort to study the process of freeze-thaw deterioration from the perspective of strain-variations in concrete. Prediction of strains is important for any modeling of concrete behavior to be complete in nature. Further, a large number of factors and conditions, e.g. temperature, physical loads, pore saturation, etc., are responsible for the variation of strain within specimens, thus making it difficult to predict. This study attempts to study the dependence of strain on various factors involved in the freeze-thaw process and takes another look at the

microscopic mechanism of freeze-thaw deterioration based on the macroscopic experimental observations.

It is further proposed here to use strains in concrete as a measure of freeze-thaw related deterioration. Since, length changes in specimens have been traditionally used to depict damage in specimens, it only makes sense to extend that understanding to strains. It is relatively easy to obtain fairly accurate strain measurements even in actual structures using embedded or surface strain-gages. Further, the measurement being in electronic in nature, can easily be transmitted to far-off locations for remote-monitoring. Here again, due to the dependence of strain on various factors, it is important to understand the individual contributions of all factors in order to obtain meaningful strain variations corrected to base conditions representing progressive damage in the structure.

This study is only a step towards achieving the above described objectives. Much more research would be required to be able to apply this study into practice. Also, this study too depends on results obtained from small specimens rather than large actual structures and on accelerated simulated environments rather than natural climate variations. However, the author believes, the findings can be extended to actual structures with more research applying test methodologies similar to that used in this study on actual structures.

## 1.2 RESEARCH SIGNIFICANCE

The aim of this research is to study the variation of strain within concrete specimens with the progress of freeze-thaw cycles. It is believed that strain variations would be an important part of any comprehensive model concerning freeze-thaw behavior of concrete and are also easy to measure even in actual structures. It is thus important to properly understand strain variations in concrete during the process. This study concentrates on sub-zero temperatures higher than -25°C. The variation of strain with temperature has been measured for specimens with various mix-proportions and of various sizes. Strain variations

within each cycle and also with progressive cycles have been studied. Specimens of various mix proportions were used to study the effect of air entrainment. Further, the effect of availability of excess water on the surface of specimens has been studied, thus outlining the dependence of these strains on water content of the specimens, availability of external water and drying and wetting of the specimens. This study takes another look at the mechanism of freeze-thaw damage in concrete in light of the observed strain variations for the given test regime. At the end, it has been proposed to use strain variations to measure damage within concrete after accounting for various factors like temperature and saturation. This research is mainly experimental in nature, though some experimental results have also been compared with simplified analytical results.

# Chapter 2

# CYCLIC FREEZE-THAW DETERIORATION: A LITERATURE REVIEW

## 2.1 BACKGROUND

Cyclic freeze-thaw deterioration is known to be the major source of deterioration of concrete in most of the places experiencing severe cold weathers. The extent of the problem can be appreciated from the fact that almost one-third of all concrete poured in Nordic European countries is susceptible to freeze-thaw deterioration (Penttala et al., 2002). Infrastructure in northern Japan has also suffered extensively due to this phenomenon (Ohta, 1991).

Damage due to freeze-thaw deterioration can take various forms, the most common being scaling and micro-cracking (Mehta and Monterio, 1997). Both these forms of damage are known to potentially progress individually within the same structural member (Marchand et al., 1995). Other forms of damage may include large-scale spalling and crumbling of concrete and crossing fatigue-like cracks visible on the surface. All these symptoms are generally accompanied by loss in strength and serviceability of concrete.

Scaling is a surface phenomenon and usually responsible for the wearing off of the outer few millimeters of concrete. Light scaling can cause concrete surfaces to become rough, and more severe scaling can expose coarse aggregate, sometimes even scaling off more than 10 mm of cover concrete. It has been found that processes like improper troweling, insufficient curing and bleeding lead to the formation of a highly porous zone of concrete near the surface that is much more

susceptible to scaling (Pigeon et al., 1996). Though its mechanism isn't very clear yet, the use of deicing salt, generally used to remove snow from pavements, bridge decks, runways, sidewalks, etc., is generally held responsible for intensified and faster scaling of concrete surface, especially in concretes with low air contents.

Tensile pressures generated within concrete, during cyclic freezing and thawing, are known to generate cracks within concrete, reducing its strength and integrity. Microscopic studies verify the growth of around 1 - 10 μm wide micro-cracks upon subjecting concrete to freeze-thaw cycles. These cracks have been found to pass through cement paste and follow the boundaries of most large aggregate particles (Jacobsen et al., 1995). Many factors are found to affect the propagation of micro-cracks within concrete, with air entrainment, water/cement ratio, strength, curing and saturation having major influence.

## 2.2 MECHANISM OF FREEZE-THAW DETERIORATION

Freeze-thaw deterioration has been historically attributed to the anomalous expansion of water upon freezing by around nine percent. The first definitive theories attempting to explain this process were given by T.C. Powers (1945, and 1949). Initially it was assumed that expansion of water within pores generates tensile pressures leading to collapse of pore walls and cracks when the pressure exceeds the tensile strength of concrete. However, damage in the form of abnormal expansion was found to occur in concrete even when pore-saturation was lower than the critical amount required to accommodate the expansion of water upon freezing. Powers proposed the theory of hydraulic pressures in which water was hypothesized to flow from the freezing sites in the outer regions of concrete, which freeze earlier than the inner parts, towards the center generating hydraulic pressures due to the resistance offered to the flow of water by viscous and surface forces (Powers, 1945).

Though initially it was out rightly rejected (Powers, 1945), a parallel was later drawn between frost-damage of concrete and frost heaving of soils as reported by

Taber (1929) and a phenomenon known as ice-accretion was proposed to account for dilatations that couldn't be accounted for by hydraulic pressures alone and (Powers and Helmuth, 1953). Experimental results carried out by many researchers supported the movement of unfrozen water from gel pores towards freezing sites due to free-energy difference between gel pores and larger cement pores. Due to high surface tension in small water droplets generating pressure on water surface, as described by the Gibbs-Thompson equation (Defay et al., 1966), the freezing point of water is found to reduce below the normal 0°C in pores of small size as in Eq. 2.1 below.

$$\ln\left(\frac{T}{T_0}\right) = -\frac{2 \cdot \Delta G \cdot \nu_w}{\Delta h \cdot r} \tag{2.1}$$

T and $T_0$ in the equation above represent the freezing temperatures for the liquid in a pore of radius r and the bulk liquid at atmospheric pressure in K respectively. $\Delta G$ represents the difference in interfacial energy between matrix and ice, and matrix and water, $\Delta h$ the latent heat of fusion and $\nu_w$ the specific volume of water.

According to this theory, water within pores would progressively freeze from the larger pores to the smaller pores at temperatures lower than 0°C. Owing to the extreme small size of gel pores, it was found that water within these pores cannot freeze at temperatures above -78°C. This leads to the generation of a steep gradient in the free energy of unfrozen water in the much smaller gel pores and ice being formed in pores nearby, thus drawing the unfrozen water from the gel pores to the freezing sites nearby. This process has been hypothesized to lead to progressive movement of unfrozen gel water into larger pores, thus leading to dilatation of concrete and finally causing cracks to grow within concrete.

Based on this theory, Powers and Helmuth (1953), explained the higher frost resistance observed for air-entrained specimens and proposed a methodology for durable mix design based on void spacing in air-entrained concrete (Powers, 1954). Though these theories having been modified through the experience of years of research and observations of actual structures (Fig.2.1), the basics remain almost the same and void spacing is one of the major factor parameter still used for

effective mix-design of air-entrained concrete (Philleo, 1983, Attiogbe, 1993, and Pleau and Pigeon, 1996). Snyder (1998) has also offered numerical analysis to evaluate the performance of these void spacing relations.

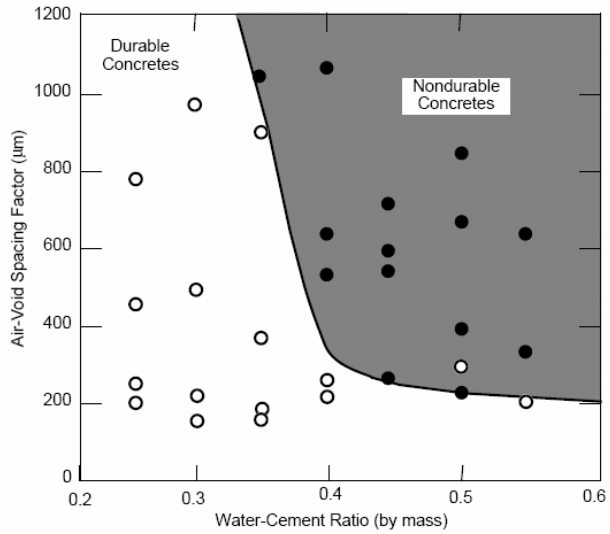


Fig. 2.1: Air-void spacing vs. water-cement ratio for a durable mix (Pigeon and Pleau, 1995, from Schulson, 1998)

Though not much experimental proof has been obtained, Kleiner (1996) has also suggested the presence of chemical processes along with mechanical processes, during the freeze-thaw process. All these theories have advanced through the years with many researchers proposing new theoretical and empirical mathematical models attempting to predict the behavior of concrete during cyclic freeze-thaw cycles like the pore-pressures (Penttala, 1998), propagation of freezing (Zuber and Marchand, 2000), and softening (Hasan et al. 2004). However, probably because of the primarily microscopic nature of the involved processes and the difficulty in observing the actual phenomenon as it happens, a perfect model for the process of freeze-thaw deterioration, which can explain all observations accurately hasn't been developed yet.

## 2.3 MAJOR FACTORS AFFECTING DETERIORATION

The extent of damage induced by subjecting concrete to cyclic freezing and thawing depends on various factors, arising from environmental conditions and material properties of concrete. In the material properties, pore properties, and

thus by extension all factors that effect pore properties, appear to play important roles in freeze-thaw deterioration. Owing probably to the fact that it is difficult to change environmental conditions for most applications, the effects of material properties on deterioration is comparatively easier to be found in literature. The following discussion looks at the major factors affecting freeze-thaw deterioration.

### 2.3.1 Water/Cement Ratio

Water/cement ratio probably has the maximum effect on pore-structure of concrete. Lower water/cement ratio is known to increase freeze-thaw durability of concrete. Along with increasing the strength of the mix, a lower water/cement ratio leads to lower porosity, permeability and pore sizes. While lower porosity reduces the amount of water in the cement paste, a lower permeability reduces the rate of water penetration into the concrete, thus increasing the freeze-thaw resistance (Detwiler et al., 1989).

### 2.3.2 Air Entrainment

As mentioned earlier, air entrainment plays a major role in freeze-thaw-resistant concrete and has now become a standard practice in cold climates. Though most research shows that around 5% to 7% by volume of concrete, lower values being ineffective, and higher reducing strength too much, is required to produce durable concrete, Powers, (1945) argued that only around 0.7% to 1% of void content in concrete, which is present even in non-air entrained concrete, would, theoretically, be able to accommodate all expansion of water in the voids. It has thus been argued that it is the void spacing, rather than the void content that controls the durability of concrete and various spacing equations have been proposed (Powers, 1949, Philleo, 1983, Attiogbe, 1993, and Pleau and Pigeon, 1996). Practical examples have also shown the importance of stable and well distributed air voids within concrete (Hulshizer, 1997).

### 2.3.3 Aggregates

Being themselves vulnerable to frost attack, porous aggregates reduce the freeze-thaw resistance of concrete. Aggregates with coarser pores but with a low total

pore volume have been reported to be more durable (Kaneuji et al., 1980). It has also been reported that concretes with smaller maximum aggregate sizes are relatively more durable (Macinnis and Lau, 1971).

### 2.3.4 Degree of Saturation

Various researches have shown concrete with low pore saturation to be less vulnerable to freeze-thaw deterioration. Certain studies have shown relatively higher freeze-thaw resistance for saturation levels lower than 80% (Fagerlund, 1977).

### 2.3.5 Curing

Higher degrees of hydration reduce the availability of freezable water within concrete pores, thus increasing the durability of concrete. Adequate curing time is thus recommended for most of the structures vulnerable to frost attack. However, accelerated steam curing is believed to result in a coarser pore-structure with higher freezable water content. Drying the concrete after the curing period would make it lesser susceptible to damage (Detwiler et al., 1989).

### 2.3.6 Freezing Rate

In his first definitive paper describing the mechanism of freeze-thaw deterioration, Powers (1945), citing experiments of other researchers, noted that higher damage has been found to occur in specimens at higher freezing rates. Pigeon et al. (1985) note that though the hydraulic pressure theory proposed by Powers is not considered valid by most researchers today, it is interesting that it can explain even relatively recent results regarding the dependence of deterioration on freezing rate. They further note that though for slower freezing rates ice-accretion would be the predominant process in action, hydraulic processes would have a more significant effect for faster freezing rates. Due to the above, since most of the laboratory freezing and thawing tests are accelerated, they would not adequately represent freezing in natural environments and it might be erroneous to assume that deterioration would be higher in rapid tests as opposed to natural freezing conditions.

## 2.4 PREVENTION OF FREEZE-THAW DETERIORATION

As discussed earlier, air-entrainment was introduced in 1930 and still is the major precautionary measure against frost-damage to concrete. In the earlier years, standard air-content in concrete was recommended to achieve acceptable frost-resistance. With the evolution of principles, minimum void-spacing is now considered as the critical factor in durable concrete (see §2.2, §2.3.2). Formation of these air bubbles and maintaining a void-spacing can however be difficult due to their instability and the interference of other agents added in concrete.

Litvan (1978, 1985) has suggested the addition of particulate porous admixtures with well defined pore-structure to the plastic mix. These particles are reported to behave as air-voids within concrete with easier and better void control and can avoid strength loss due to air-entrainment. This admixture contains particles with at least 30% porosity and pore diameters mainly between 0.8μm and 2μm, similar to the pore-sizes in air-entrained concrete and is added to concrete before mixing.

## 2.5 STRAINS DURING FREEZING AND THAWING

For any uniform isotropic linear-elastic material, the variation of strain upon the change of uniform temperature in the body can be directly calculated using the thermal coefficient of linear expansion. However, such a generalization would not hold for concrete, given its porosity and composite nature. Unrestrained strain variation in concrete upon change of temperature would in turn depend on the thermal expansions of the individual components and that in the presence of other components.

### 2.5.1 Water at Sub-Zero Temperatures

Amongst all the components of concrete, water, both in liquid and solid state, would, perhaps, have the most complex variations in volume upon change of temperature. In perfectly dry state, the behavior of concrete at low temperatures would probably be quite easy to predict. However, the presence of water in pores

with broad size ranges complicates the process due to the freezing point depression phenomenon discussed in §2.2. These pores are connected by a complex network of capillaries further adding to the complexity of the problem by allowing restrained redistribution of water within the concrete pore-structure and thus affecting the variation of strains within concrete due to its tendency to shrink upon drying.

So, it would, perhaps, make sense to begin the discussion of strain variations in concrete with the properties of water at lower temperatures. In the following discussion, experimentally obtained properties of water and ice have been presented. The data presented here has been taken from "Handbook of chemistry and physics" by Chemical Rubber Company (Lide, D.R., Ed., 2000). It should be noted here that these values are highly sensitive to the method of preparation of samples due to the occlusion of air and other gases and disagreement may be found with other literature. Figs. 2.2 to 2.4 show variation of various properties of ice and water with temperature.

The sudden change of density of water upon freezing is the main cause of freeze-thaw deterioration in concrete and leads to several other processes that cause damage. As can be seen from Fig. 2.2, there is a drastic difference between the density of ice and that of super-cooled water at the same temperature. The density of water reduces upon cooling below 0°C but that of ice if found to increase as it would for any other solid. Fig. 2.3 shows the variation of melting point of ice with pressure. An analogy can thus be drawn between freezing point depression upon application of pressure and in small pores, as discussed earlier. It should however be noted that the depression of freezing point in smaller pores is due to surface phenomenon and not due to the application of pressure. It can be seen that the pressures required to reduce the freezing point of ice even by 5°C would be tremendously excessive for concrete to bear. Also, though the thermal conductivity of ice increases rapidly and specific heat capacity reduces with reduction in temperature (Fig. 2.4), they can be considered practically constant for the temperature range considered in the current discussion.

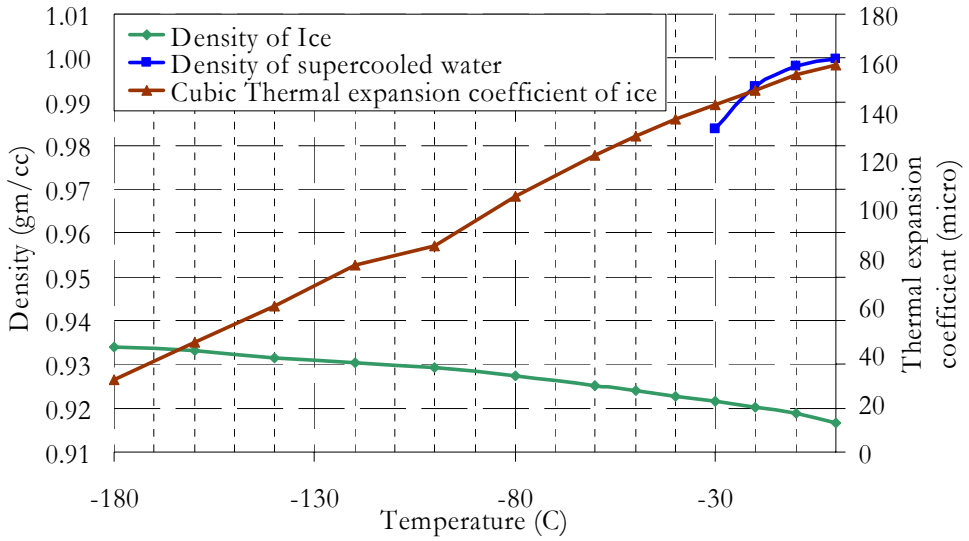


Fig. 2.2: Densities of ice and super-cooled water at sub-zero temperatures and cubic thermal expansion coefficient of ice (Lide, D.R., Ed., 2000)

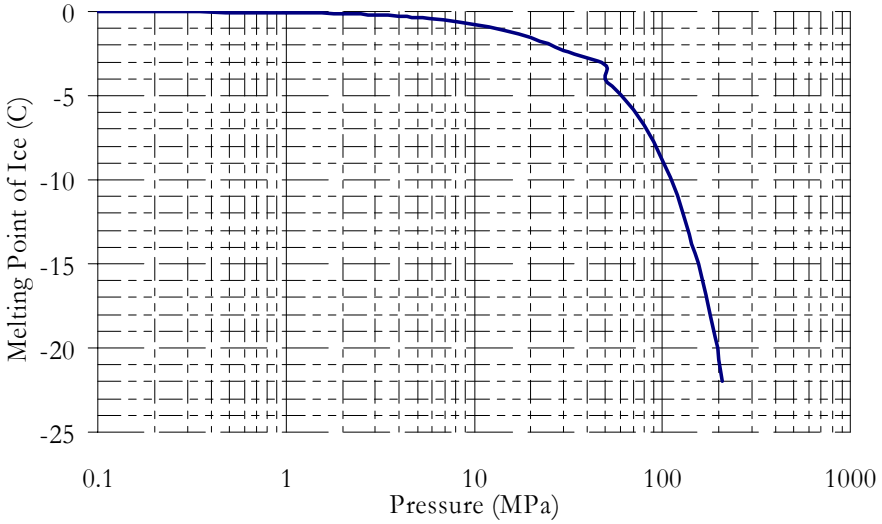


Fig. 2.3: Variation of melting point of ice with pressure (Lide, D.R., Ed., 2000)

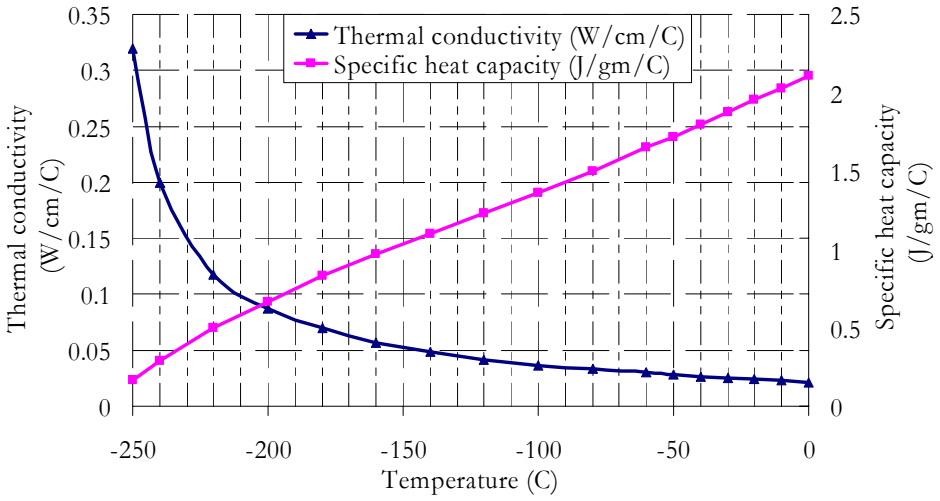


Fig. 2.4: Thermal properties of ice at sub-zero temperatures (Lide, D.R., Ed., 2000)

### 2.5.2 Previous Studies on Strain Variations

Measurement of length dilatations in concrete specimens has traditionally been reported as a measure of deterioration (Powers, 1945). Though, strain measurements appear to be a direct extension of dilatation measurements, to the authors knowledge, surprisingly little amount of work focusing on strain variations during cyclic freezing and thawing has been reported. Some of the studies reporting strains in concrete at sub-zero temperatures are discussed below.

Miura and Lee (1991) have reported experimental results dividing the strain variations with temperature into 4 major zones. At temperatures higher than -20˚C, concrete was found to follow an almost linear contraction. This was explained by the accommodation of the relatively little frozen water in the available void spaces. In the range between -20˚C and -50˚C, expansion was found to occur in concrete, reportedly due to the formation of ice in most micro-pores and the initiation of micro-cracks. At temperatures lower than -50˚C, since most of the freezable water is already frozen, concrete is reported to again exhibit a linear contraction. Upon heating back to higher temperatures, concrete strains were found to increase along a path different than during cooling and hysteresis in the strain-temperature curve was observed. Residual strains were also observed, purportedly denoting a loosened concrete structure. In this study, the residual strains and the amount of micro-cracks generated in concrete and thus the damage have been suggested to be directly related. It has also been noted that the degree of deterioration in concrete is independent of the minimum temperature if it is below -50˚C and increases with the reduction of the minimum cooling temperature in the range of -20˚C and -50˚C. The damage was reported to be insignificant at temperatures higher than -20˚C. Similar observations in length change have also been reported by MacInnis and Whiting (1979).

Pentalla (1998) has attempted to model freezing-induced pressures in wet porous materials based solely on thermodynamic relationships. Assuming equilibrium between the chemical potential of the three phases of water, a relation for pressure

exerted by freezing water when ice forms in a pore partially filled with gas and pore liquid has been suggested. This relation is shown in Eq. 2.2.

$$p - p_0 = \frac{RT}{v_i} \ln\left(\frac{p_v}{\gamma_w \chi_{unf}\, p_{v0}}\right) + \frac{\Delta h^0_{wi}}{v_i T_0}(T_0 - T) + \frac{1}{v_i}\int_{T_0}^{T}\int_{T_0}^{T} \frac{c^0_{pi} - c^0_{pw}}{T}\, dT dT \qquad (2.2)$$

Where:

p: Pressure of water

$p_0$: Reference pressure

T: Temperature

$T_0$: Reference temperature

R: Universal gas constant (8.3143 Joules per Kelvin per mole)

$v_i$: Specific volume of ice ($m^3$/mol)

$p_v$: Vapor pressure in pore system

$\gamma_w$: Activity coefficient (=1 for ideal solution)

$\chi_{unf}$: Mole fraction of pore water

$p_{v0}$: Saturated vapor pressure of liquid at p0

$\Delta h^o_{wi}$: Freezing heat of liquid at freezing temperature(J/mol)

$c^o_{pi}$, $c^o_{pw}$ : Specific heat capacities of ice and water respectively

Further, assuming the theory of linear elasticity to hold and assuming no cracks are formed; relations for strains in wet specimens were derived (Penttala and Al-Neshawy, 2002). However, a wide divergence between the experimental results and theoretical derivations was found. This divergence was attributed to cracking and non-elastic behavior of concrete as opposed to the assumptions used for this derivation and on some other thermodynamic phenomenon, which can be found in the referred study.

Hasan et al. (2004) have presented a stress-strain model of concrete damage due to cyclic freezing and thawing based on the Elasto-plastic and fracture model by Maekawa and Okamura (1983). Progressive diffusion of water into concrete during thawing has been suggested as a reason for increasing residual strains and these strains have been modeled in the form of plasticity in concrete.

Most of the studies so far have been carried out only on relatively small specimens and strain variation in larger specimens are hard to find in literature. Experiments

on large specimens subjected to high temperatures, however, indicate that strains and temperatures away from the surface would have lower variations in values and would be out of phase from the variations at the surface due to the low thermal diffusivity of concrete (Bouzoubaâ et al., 1997).

As can be seen from the above discussion, strain variations in concrete during cyclic freezing and thawing are still not well understood leaving many holes in current knowledge about the phenomenon. The current research attempts to study various phenomenon associated with cyclic freeze-thaw deterioration and their effect on strain variations in concrete. As mentioned earlier, this study too concentrates on relatively small sized specimens but it is believed that with some research, the results from this study can be applied to actual structures. The test regime here is limited to temperatures higher than -25°C, considering the practical conditions for most locations. The variation of strains with temperature has been studied for specimens of different sizes and mix proportions. The experimental conditions vary a little for different specimens, but the minimum center temperatures for most of the specimens lie in the range of -20°C to -25°C. The effect of presence of water on specimen surface has also been studied.

## 2.6 PORE-STRUCTURE OF CONCRETE AND DRYING SHRINKAGE

It shall be seen in the subsequent discussion that drying shrinkage plays an important part in the process of cyclic freezing and thawing. A small discussion on drying shrinkage would thus be presented here. Two main kinds of pore spaces, viz. Capillary Pores and Gel Pores, are known to be present in concrete micro-structure (Mehta and Monteiro, 1997). The capillary pores are the spaces unfilled by the hydrated cement paste. In the initial stages of hydration, these pores may be as large as several micrometers (μm) and later shrink to sizes varying between few tens of nanometers (nm). The gel pores, however, have a much smaller size, suggested to be around 5 to 20 Å. This space is the inter-layer spacing within the C-S-H microstructure and contains strongly bound water which cannot be removed unless subjected to extreme drying (Maekawa et al., 1999). However, this

water is known to migrate to the larger capillary pores during freezing due to a process called ice-accretion as discussed in §2.2.

It has been found that removal of this strongly held water from the gel pores under drying conditions causes dimensional instabilities in hydrated cement paste and leads to shrinkage of concrete. A similar removal of this inter-layer water upon high loading is also known to contribute to creep in concrete. It is also seen that shrinkage is not fully recoverable upon wetting after the first drying reportedly due to formation of new bonds in C-S-H structure where the water was earlier held. In the following discussion, another look shall be taken on the mechanism of freeze-thaw deterioration, considering the drying of gel pores due to ice-accretion, based on experimental observations of strain-variations in concrete. The subsequent chapters discuss the experiments carried out, their results and the conclusions made from this study.

# Chapter 3

# EXPERIMENTS: PROCEDURES, CONDITIONS AND BRIEF OVERVIEW OF RESULTS

This study concentrates on measurement of strains in concrete specimens when subjected to accelerated cyclic freezing and thawing to temperatures around -20˚C to -25˚C. The experiments were carried out in two main series and further smaller experiments. The first series was used as the pilot series and the subsequent experiments were designed based on the results from the previous set of experiments. Consequent experiments were thus designed in order to make clear specific findings of the preceding series. The following discussion presents the specifics of the experiments and brief overviews of the results obtained. A detailed discussion of all the results shall follow in subsequent chapters.

## 3.1 SERIES 1: TEMPERATURES AND STRAINS

This series was designed to study the variation of temperatures and strains in specimens of 3 different sizes. While strain was measured for one specimen of each size for only a single mix proportion, temperatures were measured in specimens of the three sizes for three different mix proportions. In this series the specimens were subjected to 4-hour rapid freeze-thaw cycles with the temperature of the thermal exchange medium varying between +20˚C and -25˚C.

### 3.1.1 Specimen Specifications

#### *3.1.1.1 Materials Used*

The specimens were prepared using concrete mixed in the laboratory using Sumitomo brand Ordinary Portland Cement (OPC) from Osaka, Japan. Tables 3.1

and 3.2 show the ignition loss in the cement, oxide composition of the cement by chemical analyses, the potential compound composition, i.e. the calculated amounts of complexes using experimentally obtained oxide compositions and other properties of the OPC used. These values have been obtained from tests performed by the cement manufacturer.

Table 3.1: Composition of cement

| **Item** | ig.loss | $SiO_2$ | $Al_2O_3$ | $Fe_2O_3$ | CaO | MgO | $SO_3$ | $Na_2O$ |
|---|---|---|---|---|---|---|---|---|
| **Percentage** | 0.77 | 20.84 | 5.95 | 2.62 | 63.63 | 1.79 | 1.97 | 0.18 |
| **Item** | $K_2O$ | $TiO_2$ | $P_2O_5$ | MnO | $C_3S$ | $C_2S$ | $C_3A$ | $C_4AF$ |
| **Percentage** | 0.33 | 0.34 | 0.08 | 0.1 | 51.2 | 21.2 | 11.3 | 8 |

Table 3.2: Properties of cement

| **Density ($g/cm^3$)** | **Fineness ($cm^2/g$)** | **Setting time** | | | **Compressive strength ($N/mm^2$)** | | |
|---|---|---|---|---|---|---|---|
| | | **Water (%)** | **Initial (hh-mm)** | **Final (hh-mm)** | **3days** | **7days** | **28days** |
| 3.15 | 3470 | 26.7 | 01-51 | 03-00 | 29 | 43 | 60.5 |

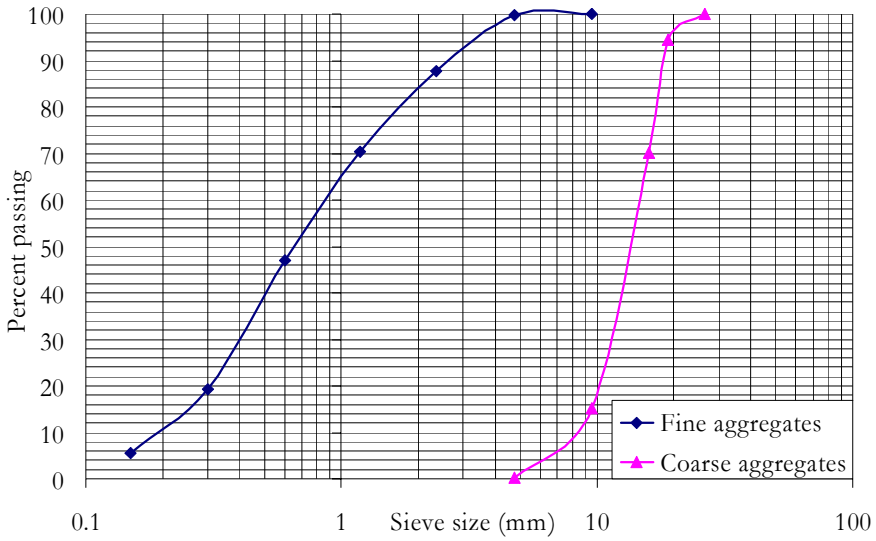


Fig. 3.1: Particle size distribution of aggregates

Fine aggregate (FA) from Fuji River, Japan, with a density of 2.63 $gm/cm^3$ and absorption coefficient of 2.19%, was used in the mix. 20 mm $G_{max}$ crushed coarse aggregate (CA), procured from Ryojin village in Saitama Prefecture, Japan, with a dry density of 2.73 $gm/cm^3$ and absorption coefficient of 0.57% was used. The particle size distributions of the aggregates are shown in Fig. 3.1. These values were obtained by tests in the laboratory.

### *3.1.1.2 Mix Design*

Table 3.3 shows the design of the concrete mixes used in this series of experiments. The admixtures are denoted as percentage by weight of cement. The strength was measured after 13 weeks of under-water curing at 20°C, one day after the start of the freeze-thaw cycles. The names of the chemical admixtures are according to the coding of the manufacturer NMB Corporation, Japan. 78S is an AE water-reducing agent, SP8SE a super-plasticizer and 303A the air-entraining agent. The coding of the mixes has been done according to their water-cement ratio and whether or not air was entrained, with E standing for air-entrained concrete and U for un-entrained concrete.

Table 3.3: Unit (1 $m^3$) composition of concrete in Series 1

| Mix No. | Water (kg) | OPC (kg) | FA (kg) | CA (kg) | Water Reducer | Air Agent (303A) | Air | Strength (MPa) |
|---|---|---|---|---|---|---|---|---|
| M-55-E | 160 | 291 | 826 | 1032 | 78S – 1.1% | 0.6% | 7% | 39.8 |
| M-55-U | 160 | 291 | 861 | 1077 | 78S – 2.2% | 0 | 1.2% | 55.4 |
| M-40-E | 160 | 400 | 785 | 981 | SP8SE – 0.5% | 0.6% | 6.5% | 55.3 |

### *3.1.1.3 Specimens: Design and Coding*

In this series of experiments a total of 24 cuboidal plain concrete specimens of three sizes were cast as shown in Table 3.4. As can be seen from the table, three specimens, coded 7-55-E-M, 10-55-E-M and 15-55-E-M had mold strain gauge cast at their center. This sensor is well suited to obtain electronic readings of strain and temperature within concrete due to its extremely low elastic modulus of 40MPa and water-proof construction. 13 other specimens had a total of 38 thermocouples cast within them to measure temperatures within the specimens at various locations. The thermocouples were located along a diagonal of the cross-section of the specimen located at the center along the length. In order to avoid congestion of wires within the concrete and considering the symmetry of the specimens, thermocouples at similar locations within specimens were avoided. In some cases, two similar specimens of same mix proportions were fitted with thermocouples at different locations to obtain temperature readings at closer intervals. When such a pair of specimens was present, the thermocouples in one

of the specimens were positioned such that the innermost thermocouple was at the center (centered placing), while in the other one it was away from the center by half the spacing between the sensor locations (off-center placing). Fig. 3.2 shows the placing of the sensors within the specimens for easier understanding. All sensors were connected to an automatic data-logger during the freeze-thaw cycles, recording readings at a regular interval of 5 minutes. Apart from the above mentioned specimens, 8 more plain concrete specimens with no sensors cast within were used as references to check for any observable effect of sensors on specimen behavior.

Table 3.4: Details of specimens in Series 1

| S.no. | Specimen code | Mix no. | Size (cm) | Sensor type (number) | Distance (cm) from center for sensor no. | | | |
|---|---|---|---|---|---|---|---|---|
| | | | | | 1 | 2 | 3 | 4 |
| 1 | 7-55-E-M | M-55-E | 7x7x38 | Mold Gauge(1) | 0.0 | | | |
| 2 | 7-55-E-3 | | | Thermocouple(3) | 0.0 | 2.0 | 4.0 | |
| 3 | 7-55-E-0 | | | None | | | | |
| 4 | 10-55-E-M | | 10x10x38 | Mold Gauge(1) | 0.0 | | | |
| 5 | 10-55-E-3 | | | Thermocouple(3) | 0.0 | 2.5 | 5.0 | |
| 6 | 10-55-E-0 | | | None | | | | |
| 7 | 15-55-E-M | | 15x15x38 | Mold Gauge(1) | 0.0 | | | |
| 8 | 15-55-E-4 | | | Thermocouple(4) | 0.0 | 2.5 | 5.0 | 7.5 |
| 9 | 15-55-E-0 | | | None | | | | |
| 10 | 7-55-U-3 | M-55-U | 7x7x38 | Thermocouple(3) | 0.0 | 2.0 | 4.0 | |
| 11 | 7-55-U-2 | | | Thermocouple(2) | 1.0 | 3.0 | | |
| 12 | 7-55-U-0 | | | None | | | | |
| 13 | 10-55-U-3 | | 10x10x38 | Thermocouple(3) | 0.0 | 2.5 | 5.0 | |
| 14 | 10-55-U-2 | | | Thermocouple(2) | 1.25 | 3.75 | | |
| 15 | 10-55-U-0 | | | None | | | | |
| 16 | 15-55-U-4 | | 15x15x38 | Thermocouple(4) | 0.0 | 2.5 | 5.0 | 7.5 |
| 17 | 15-55-U-4F | | | Thermocouple(4) | 1.25 | 3.75 | 6.35 | 8.75 |
| 18 | 15-55-U-0 | | | None | | | | |
| 19 | 7-40-E-3 | M-40-E | 7x7x38 | Thermocouple(3) | 0.0 | 2.0 | 4.0 | |
| 20 | 7-40-E-2 | | | Thermocouple(2) | 1.0 | 3.0 | | |
| 21 | 7-40-E-0 | | | None | | | | |
| 22 | 10-40-E-3 | | 10x10x38 | Thermocouple(3) | 0.0 | 2.5 | 5.0 | |
| 23 | 10-40-E-2 | | | Thermocouple(2) | 1.25 | 3.75 | | |
| 24 | 10-40-E-0 | | | None | | | | |

The first three denominations in the coding of the specimens denote the size of the specimen, water-cement ratio, and air-entrainment respectively. The last

denomination indicates the sensor included within the specimen, with an 'M' indicating a mold gauge and a number denoting the number of thermocouples cast inside the specimens. The specimens with the last denomination as '0' had no sensor cast within. A 'F' was added to the end of specimen number 17, coded 15-55-U-4F, having off-center thermocouple placing, to differentiate it with specimen number 16, coded 15-55-U-4, having centered thermocouple placing.

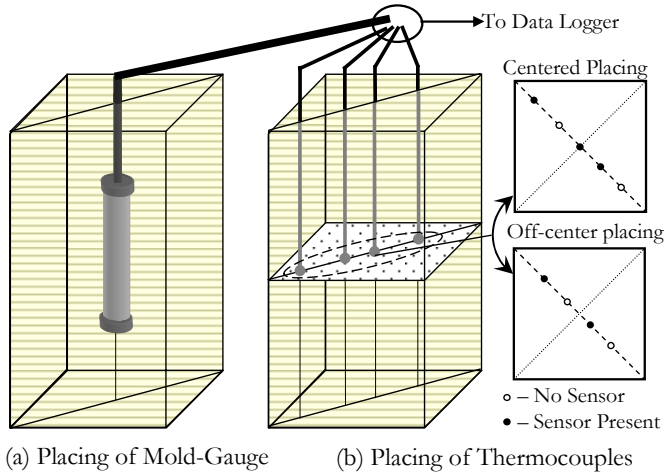


Fig. 3.2: Placing of sensors

#### *3.1.1.4 Curing and pre-test conditions*

The specimens were cured for a total period of about 13 weeks. The specimens were under water for initial 11 weeks and had to be removed at that time for transportation. The specimens were cushion wrapped during transportation to protect them from any jerks and mishandling. During this period of around 40 hours, the specimens were subjected to normal air conditions and were kept in a curing chamber with humidity 60% and temperature 20°C for the subsequent 12 days. The specimens were then moved to the test chamber and placed within rubber sleeves filled with water till 1-2 cm above the specimen tops.

### 3.1.2 Freeze-Thaw Cycles: Test Conditions

#### *3.1.2.1 Wet Cycles*

The experimental setup consisted of three main segments: 'Temperature Control', 'Environment Chamber', and 'Data Recording', as shown in Fig. 3.3. The

specimens were placed inside rubber sleeves and then placed in the environment chamber. The sleeves were filled with water till 1-2 cm above the specimen tops. It is due to the presence of this water around the specimens that these cycles would be referred to as "Wet Cycles". The chamber was filled with Ni-Brine, a thermal exchange fluid, to levels higher than the level of water in the sleeves. The temperature of the exchange fluid was controlled electronically according to a pre-programmed schedule. In each cycle of four hours, the temperature of the medium was reduced to -25°C in the first two hours and then increased back to 20°C in the next two hours. The heating and cooling rates were different and were automatically set by the temperature control segment. Fig. 3.4 shows the temperature variations in the exchange medium in a typical four-hour cycle.

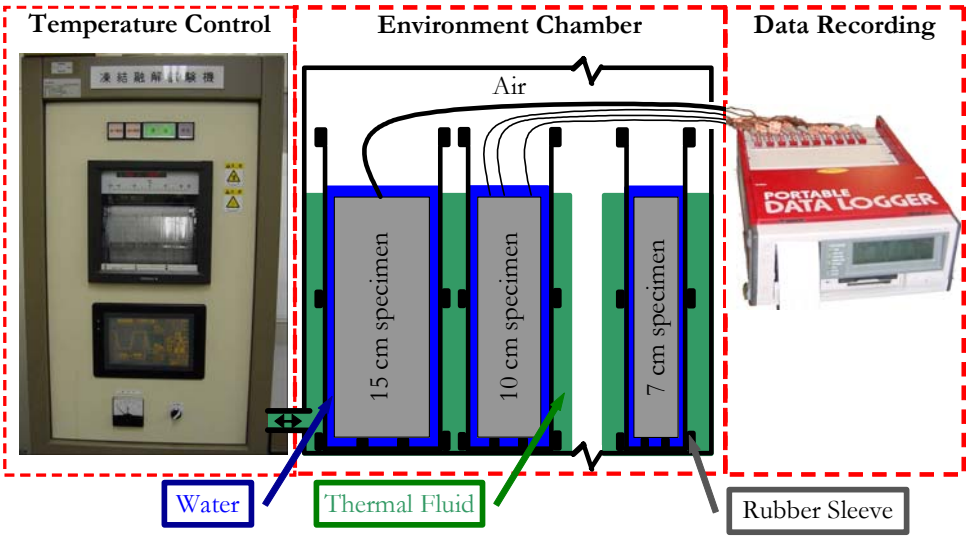


Fig. 3.3: Experimental setup

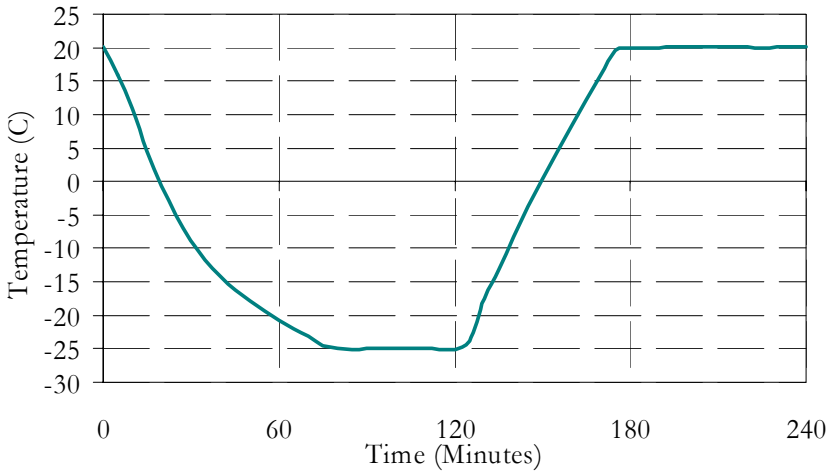


Fig. 3.4: Typical temperature variation in thermal exchange fluid in Series 1

At the end of every 36 cycles, the specimens were removed from the chamber and weighed and their relative dynamic modulus was measured. During this period the specimens were subjected to room conditions for three to four hours each time. In this period, the sensors were disconnected from the recording apparatus and strains and temperatures were not recorded. The temperature of the specimens was brought up to about 20°C at the end of each set of cycles to ease handling. Each set of 36 cycles was carried out in one week, with the cycles lasting for six days and the last day used for reheating the specimens to room temperature and for measurements. The specimens were replaced in the environment chamber and the sleeves were refilled with water after the measurements. The sensors were then reconnected to the recording apparatus.

#### *3.1.2.2 Dry Cycles*

At the end of nine above described sets of 36 wet cycles, making for a total of 324 cycles, another 36 similar cycles were carried out without pouring any water into the sleeves. These cycles would be referred to as the dry cycles owing to the absence of water around the specimens.

### 3.1.3 Experimental Errors and Imperfections

#### *3.1.3.1 Exposure Differences*

It must be pointed out here that though the specimens were placed in the environment chamber together, thus subjecting the sleeves of all sizes to approximately same conditions, the temperature conditions within the sleeves varied extremely due to the difference in the size of the sleeves and thus the amount of water or air present around the specimens. The extent of exposure thus varied with the size of the specimen. As an example, Fig. 3.5 shows the temperature variation within the sleeve of one specimen of each size. These temperatures can be considered as the temperatures on the surface of the specimens for all practical purposes. As is apparent from the figure, 10 cm specimens were subjected to the most severe conditions while the conditions for the 15 cm specimens were the least severe. The difference in the temperatures between different sleeves of the same size was insignificant.

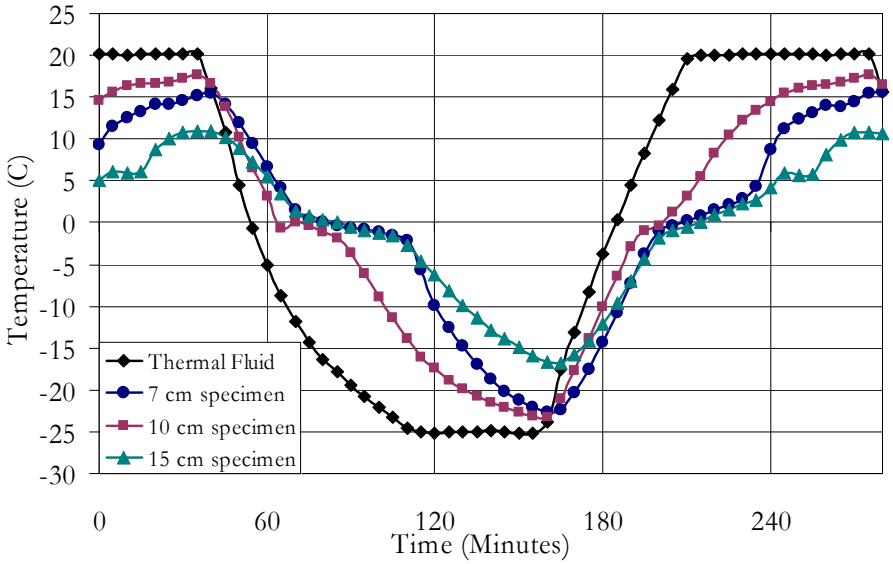


Fig. 3.5: Difference in surface conditions for different specimen sizes

#### *3.1.3.2 Initial Water Gain*

Even though the specimens were kept submerged in water for around 1 day before the freeze-thaw cycles were started and after moving it from the 60% humidity chamber, the specimens may not have been saturated to the extent they would be if they had been submerged in water for a much prolonged period. So, some permeation of water into the specimens might have taken place during the freeze-thaw cycles due to change in humidity outside. This might have lead to both weight-gain and a rise in strain within the specimens.

#### *3.1.3.3 Drying During Measurements*

Since the specimens were removed from controlled conditions after every 36 cycles, and were subjected to room conditions for the period their weight and relative dynamic modulus was measured, some unquantifiable amount of water was lost from the specimens in this period. There would hence be some loss in weight and reduction in strains within the specimens within this period, depending on the room conditions that day and the length of time they had been removed from the chamber. This change in strain can however be quantified from the readings before and after the measurements. Also, it is believed that only if the weight loss in specimens is small would this cause a significant difference in the actual and measured weight loss in the specimens.

#### *3.1.3.4 Lost Data*

The data between cycles 289 and 324 was lost beyond recovery due to hardware malfunction. Only the readings for the initial part of the 289th cycle and at the end of the 324th cycle could be obtained.

### 3.1.4 Results

#### *3.1.4.1 Weight Loss and Relative Dynamic Modulus*

Table 3.5 lists the percentage weight loss and percentage loss in young's dynamic modulus for the specimens at the end of 324 freeze-thaw cycles. As mentioned in §3.1.3.2, a gain in weight was observed for all specimens after the first 36 cycles possibly due to excessive penetration of water into the specimens upon being submerged in water after being kept in 60% percent humidity chamber. Also, since the damage in the specimens in the first 36 cycles was quite small, the loss in weight due to scaling was lower than the gain in weight due to water absorption leading to an overall increase in the weight of the specimens. So, to prevent disproportionate weight gains being reflected in the results, weight losses have been presented as compared to the weights at the end of 36 cycles. The final weight loss values so calculated were found to vary between 0.01% and 1.89%. Weight losses were observed to be relatively higher in specimens without entrained air.

Table 3.5: Weight loss (WL) and relative dynamic modulus (RDM)

| **Sp. code** | 7-55-E-M | 7-55-E-3 | 7-55-E-0 | 10-55-E-M | 10-55-E-3 | 10-55-E-0 |
|---|---|---|---|---|---|---|
| **WL (%)** | 0.83 | 0.99 | 0.85 | 0.48 | 0.60 | 0.88 |
| **RDM (%)** | 102.7 | 103.0 | 102.4 | 102.4 | 102.6 | 100.8 |
| **Sp. code** | 15-55-E-M | 15-55-E-4 | 15-55-E-0 | 7-55-U-3 | 7-55-U-2 | 7-55-U-0 |
| **WL (%)** | 0.71 | 0.69 | 0.01 | 1.55 | 1.28 | 1.39 |
| **RDM (%)** | 97.3 | 97.1 | 103.0 | 102 | 102.4 | 100.0 |
| **Sp. code** | 10-55-U-3 | 10-55-U-2 | 10-55-U-0 | 15-55-E-0 | 15-55-U-4 | 15-55-U-4F |
| **WL (%)** | 1.55 | 1.25 | 1.10 | 1.29 | 1.37 | 1.89 |
| **RDM (%)** | 98.9 | 99.9 | 100.9 | 101.8 | 99.9 | 102.8 |
| **Sp. code** | 15-55-U-0 | 7-40-E-3 | 7-40-E-2 | 7-40-E-0 | 10-40-E-3 | 10-40-E-2 |
| **WL (%)** | 0.37 | 0.33 | 0.31 | 0.20 | 1.36 | 0.28 |
| **RDM (%)** | 100.26 | 100.1 | 100.49 | 101.6 | 101.2 | 99.6 |

It can also be seen from the relative dynamic modulus listed in the table that the damage in the specimens was relatively small with most of the final values distributed fairly randomly distributed between ±3% of the original values. Though a small increase in the dynamic modulus was noticed in many specimens, since the increase is small, it can be attributed to experimental and human errors. As can also be seen in Fig. 3.6, the weight loss and relative dynamic modulus values of the specimens show the low extent of damage in the specimens even at the end of over 300 freeze-thaw cycles.

Fig. 3.6: Specimens 7-55-E-M, 10-55-E-M and 15-55-E-M at the end of all cycles

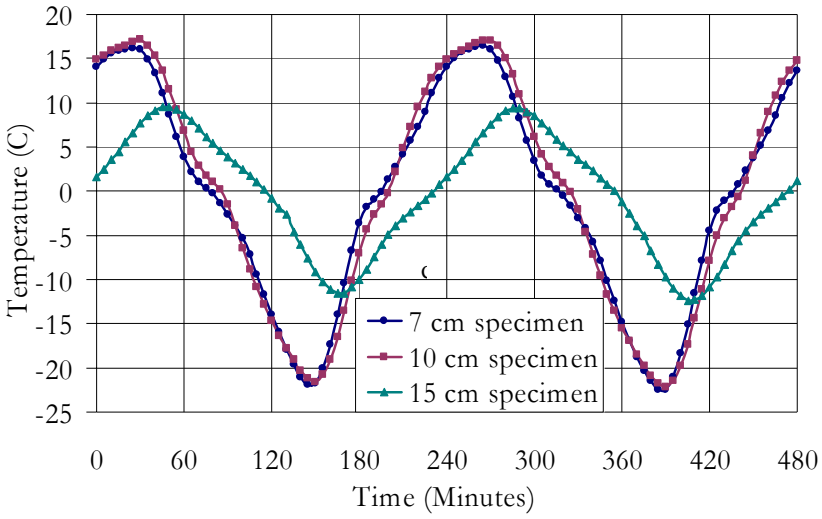


Fig. 3.7: Temperature variations at center of specimens during wet cycles

### *3.1.4.2 Temperature Variations*

Data from all temperature sensors was read into an automatic data-logger at an interval of 5 minutes. Since the temperatures were different on the surface of

specimens of different sizes, these temperatures cannot be compared directly. As can be seen from Fig. 3.7, the temperature variations at the center of the 7 cm and the 10 cm specimens were almost the same and the temperature ranges in the 15 cm specimens were relatively shorter due to different surface conditions for the different specimens as shown in Fig. 3.5.

Fig. 3.8 shows that the temperature variations at the center of the 10 cm specimens were found to be largely the same irrespective of the mix-proportions. A similar correspondence was noticed in the specimens of other sizes (Fig. 3.9). It can thus be concluded that, in the current test regime, the thermal diffusivity of concrete is largely independent of its mix proportions.

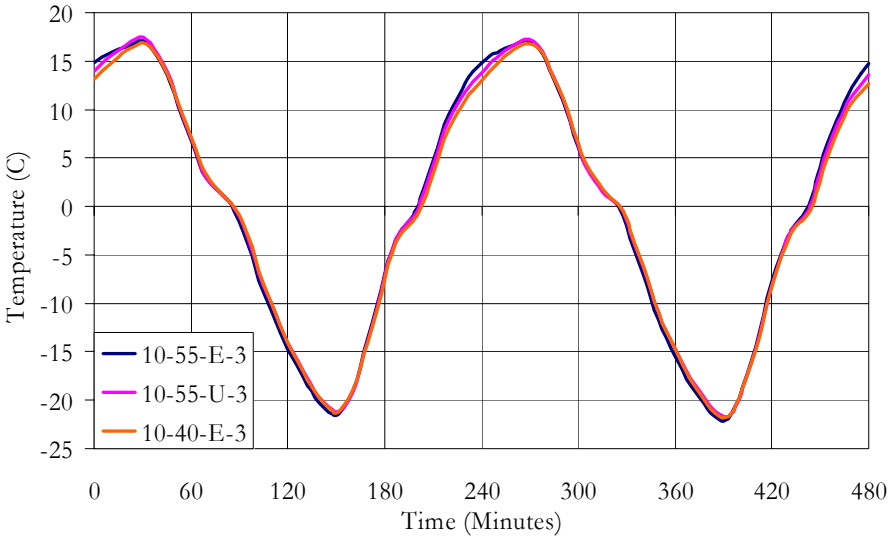


Fig. 3.8: Temperature variations in 10 cm specimens of different mix-proportions

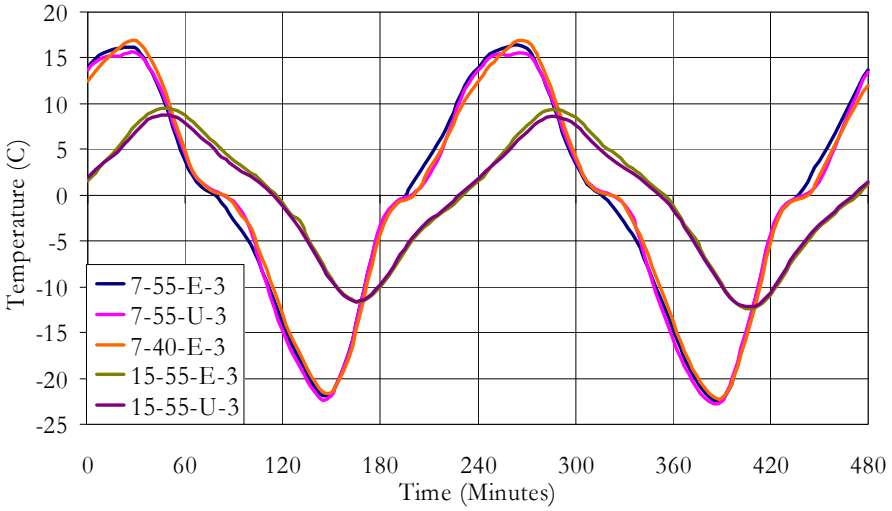


Fig. 3.9: Temperature variations in 7 cm and 15 specimens of different mix-proportions

The temperature ranges within the specimens were found to reduce during the dry cycles since thermal exchange becomes slower due to the lower thermal diffusivity of air when compared to water. Typical temperature variations at the center of the specimens for a dry cycle are shown in Fig. 3.10. Upon the analysis of these results using FEM transient thermal analysis tools, the thermal diffusivity (D) of concrete was found to be $7.27\times10^{-7}$ m²/sec. This value has been used in further analysis.

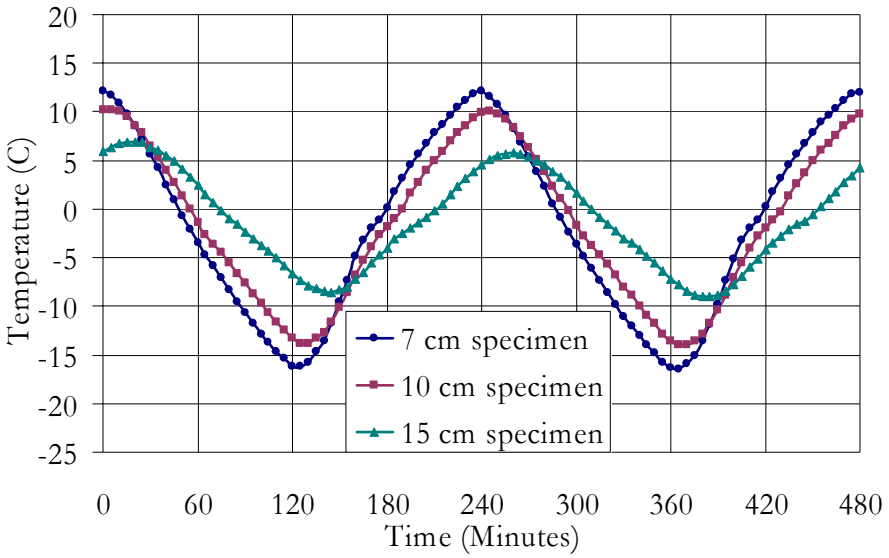


Fig. 3.10: Temperature variations at center of specimens during dry cycles

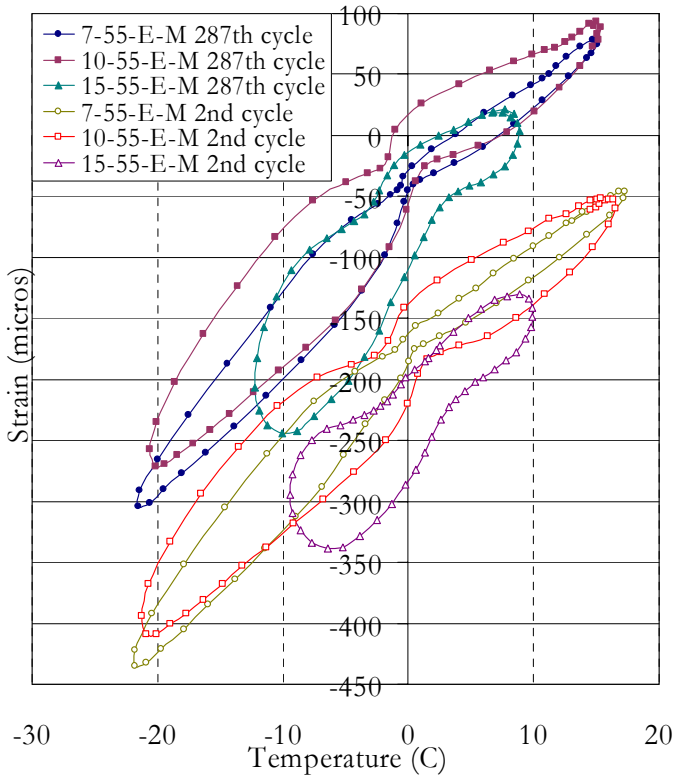


Fig. 3.11: Variation of strains against temperature during wet cycles

### *3.1.4.3 Strain Variations*

Fig. 3.11 shows the strain-temperature behavior for the three specimens in the first and the 287th cycle. The values of strains were set to 0μ at 25.5˚C before the start of the first freeze-thaw cycle. The first observable feature of the curve is the hysteresis between the strain variations with temperature. The strain at the same temperature was higher during thawing when compared to freezing. Also, the area within the hysteresis curve can be seen to be higher for larger specimens.

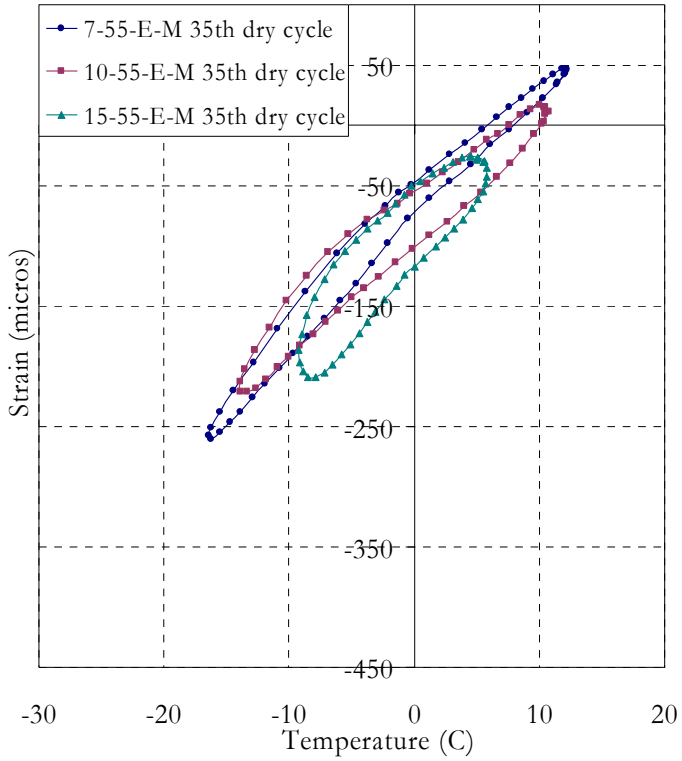


Fig. 3.12: Variation of strains against temperature during dry cycles

When compared to the strain-temperature behavior during dry cycles, shown in Fig. 3.12, the main difference can be seen in the presence of a kink near 0˚C during wet cycles showing that the feature is present because of freezing of the water around concrete. During freezing, due to the high latent heat of fusion of water, the temperature of water stops at 0˚C till all water freezes or melts, even as the heat exchange continues. The water in the sleeves would freeze and melt at a temperature close to 0˚C, thus preventing the temperature to change until the freezing or melting has completed. As the temperature on the surface of the specimen remains constant for this period, the thermal gradients within start to reduce, thus releasing the thermal gradient induced stresses within the specimens.

The strains would thus reduce during thawing and increase during freezing, creating the kink observed in the strain-temperature curves for specimens submerged in water. Both, the effect of size on the hysteresis behavior and the above discussion indicate that thermal gradients within the specimens have a major effect on the observed hysteresis.

Another noticeable feature in the curves is the upward migration of strains if measured at the same temperature. It can be seen, from the 2nd and 287th cycles, that though the approximate shape of the strain-temperature curves remains the same, there is a shift in the curves such that the strain increases with the progress of freeze-thaw cycles. This change in strain, when measured at the same temperature, with the progress of cyclic freezing and thawing is henceforth referred to as "Residual Strain".

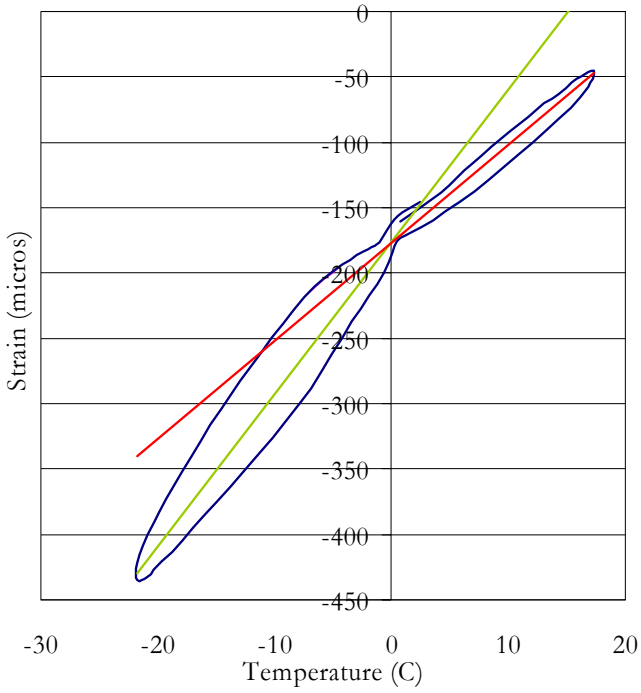


Fig. 3.13: Higher apparent thermal expansion coefficient below 0°C

Though the strain-temperature behavior is not perfectly linear, a comparison of average slopes in the positive and negative temperature regions shows a higher strain-temperature rate below 0°C. This strain-temperature rate can be referred to as the apparent thermal expansion coefficient ($\alpha_{app}$) since it represents the fractional change in length of the specimens upon inducing a 1°C temperature

change in the specimen. Fig. 3.13 shows the difference in the average apparent thermal expansion coefficients for the 7 cm specimen. A similar variation can be observed in the strain-temperature behavior of the larger specimens.

The strain variations and apparent thermal expansion coefficient of individual specimens have been discussed further in subsequent chapters.

## 3.2 SERIES 2: EFFECT OF WATER INGRESS

This series of experiments was designed based on the results of Series 1. In this series, strain variations were measured at the center of seven specimens of two mix proportions and two sizes. The specimens were subjected to freeze-thaw cycles similar to Series 1, with the temperature in the thermal exchange fluid varying between +10°C and -25°C, and the effect of availability of water on the specimen surface was studied. The raw materials and strain-gauges used in the preparation of the specimens in this series were the same as that used in Series 1. The following discussion deals with the details of the specimens, the test conditions and a brief overview of the obtained results.

### 3.2.1 Specimen Specifications

#### *3.2.1.1 Mix Design*

Table 3.6 shows the design of the two concrete mixes used in this series of experiments. The strength was measured after 28 days of under-water curing at 20°C, two days before the start of freeze-thaw cycles. The coding of the mixes, similar to Series 1, depends on the water-cement ratio and the presence or absence of air-entrainment, E denoting air-entrained and U un-entrained concrete.

Table 3.6: Unit (1 $m^3$) composition of concrete in Series 2

| Mix No. | Water (kg) | OPC (kg) | FA (kg) | CA (kg) | Water Reducer | Air Agent (303A) | Air | Strength (MPa) |
|---|---|---|---|---|---|---|---|---|
| M-65-U | 185 | 285 | 927 | 948 | 78S – 1.0% | 0.0% | 1.0% | 37.6 |
| M-65-E | 165 | 249 | 895 | 992 | 78S – 1.1% | 1.0% | 7.0% | 23.0 |

Table 3.7: Details of specimens in Series 2

| S.No. | Specimen code | Mix No. | Size (cm) | Exposure condition |
|---|---|---|---|---|
| 1 | 7-65-U-M-A | M-65-U | 7x7x36 | Wet throughout |
| 2 | 7-65-U-M-B | | | Alternating wet and dry |
| 3 | 10-65-U-M-A | | 10x10x36 | Wet throughout |
| 4 | 10-65-U-M-B | | | Alternating wet and dry |
| 5 | 10-65-U-M-C | | | Dry throughout |
| 6 | 10-65-E-M-A | M-65-E | 10x10x36 | Wet throughout |
| 7 | 10-65-E-M-B | | | Alternating wet and dry |

#### *3.2.1.2 Specimens: Design and Coding*

Seven main specimens were used in this series of experiments. The details of the specimens and their exposure conditions during the freeze-thaw cycles are shown in Table 3.7. All these specimens had mold strain gauges cast at their center. The coding of these specimens is similar to Series 1, with the first three denominations denoting the size of the specimen, water-cement ratio, and air-entrainment respectively and the fourth denoting the mold strain gauge. The last, fifth, denomination denotes the exposure condition of the specimens during the freeze-thaw cycles. These exposure conditions shall be discussed further in later sections.

#### *3.2.1.3 Curing and pre-test conditions*

The specimens were first cured submerged under water for a total period of 15 days. At the end of these 15 days, the specimens were wrapped and transported being removed from water for around 24 hours. The specimens were then placed inside the testing chamber inside rubber sleeves, with water filled around the specimens, for a period of 14 days before the freeze-thaw cycles were started. The temperature of the water around the specimens varied between 17°C and 20°C in this period.

### 3.2.2 Freeze-Thaw Cycles: Test Conditions

The same experimental setup and recording apparatus as in Series 1 was used in this series. The temperature of the thermal exchange fluid in this series was varied between 10°C and -25°C. The temperature range was reduced in this series so as to concentrate on the sub-zero part of the cycles and to attain higher damage in

the specimens considering that proper thawing in the specimen would occur by raising the temperature to around 5°C. The time period of the first 72 cycles was set at 4 hours and was increased to 4 hour 15 minutes for the remaining 242 cycles of the total 314 cycles carried out. The time period of the cycles was increased so as to obtain further lower temperatures while freezing. The temperature ranges in the first two cycles were shorter than the set values. Fig. 3.14 shows the typical temperature variations in the thermal exchange fluid during the freeze-thaw cycles.

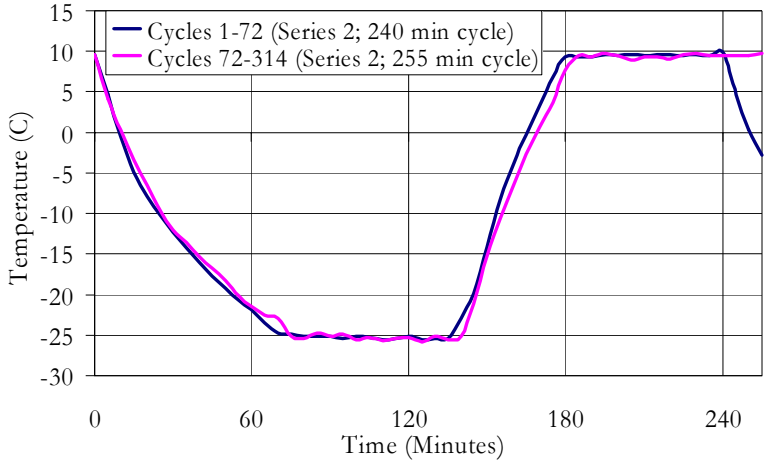


Fig. 3.14: Typical temperature variation in thermal exchange fluid in Series 2

Like Series 1, the experiments were carried out in sets of 36 cycles. At the end of every 36 cycles, the temperature of the specimens was brought up to 15°C to ease handling and their weights and relative dynamic modulus were measured. During this period the specimens were subjected to normal room conditions for a period of about 4 hours each time. The gauges were disconnected from the recording apparatus during the measurements and readings were not made during this period. After the measurements were made, the specimens were replaced in the environment chamber and reconnected to the recording apparatus.

Three different moisture conditions around the specimens were used in this series of experiments. For condition A, water was filled into the sleeves up to around 1-2 cm above the upper surface of the specimen throughout the entire 314 freeze-thaw cycles. In condition B, the moisture condition was alternated between wet and dry through the cycles as shown in Table 3.8, wet being when water was

present inside the sleeves during the cycles and dry when water was not poured into the sleeves. For the specimens under condition C, water was not poured inside the sleeves throughout the 314 test cycles. The table also lists the equivalent number of days for the cycles. Due to discontinuity in cycles, some data will be presented against number of days from the start of cycles.

Table 3.8: Specimen states for B type exposure condition

| **Days** | 0-7 | 7-14 | 14-21 | 21-28 | 28-42 | 42-49 | 49-56 | 56-63 |
|---|---|---|---|---|---|---|---|---|
| **Cycle Nos.** | 1-36 | 37-72 | 73-108 | 109-144 | 145-206 | 207-242 | 243-278 | 279-314 |
| **No. of Cycles** | 36 | 36 | 36 | 36 | 62 | 36 | 36 | 36 |
| **State** | Wet | Dry | Wet | Dry | Wet | Dry | Wet | Dry |

Like Series 1, the effect of mix-proportion on temperature variations was observed to be insignificant. Fig. 3.15 shows the temperature variation at center of specimens during typical wet and dry cycles for both specimen sizes.

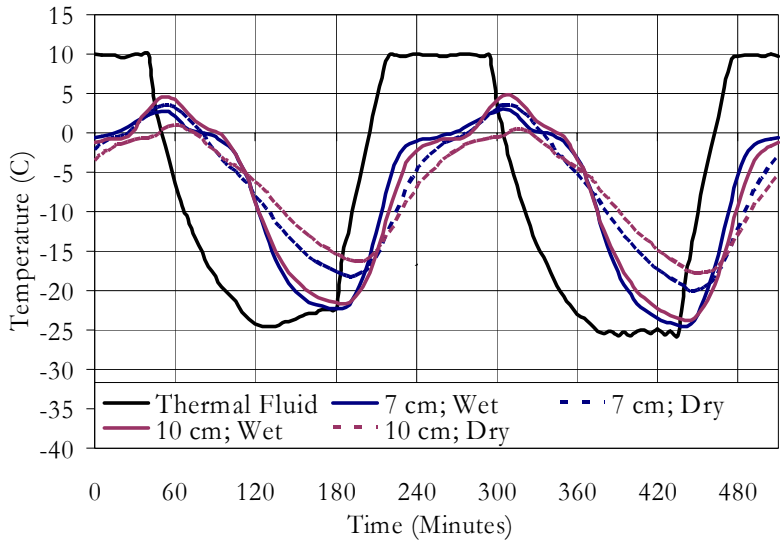


Fig. 3.15: Typical temperature variations at center of specimens in Series 2

### 3.2.3 Experimental Errors and Imperfections

The conditions described from §3.1.3.1 to §3.1.3.3 in Series 1 are also applicable for Series 2 with applicable differences in conditions between Series 1 and 2, as previously described in §3.2. Also, due to technical problems, the freeze-thaw cycles were stopped after 26 cycles from the start of 144th cycle (after 170th cycle) when the B-type exposure condition specimens were in wet state. The temperature of the thermal fluid at this point was around 3°C and then increased

linearly to around 10°C in the following 54 hours that the cycles were discontinued. The cycles were continued after this intermission with the specimens continuing to be in the state they were in the previous 26 cycles and 36 more cycles were carried out. Due to this, there is a discontinuity in the exposure condition for the B-type exposure condition specimens, with a continuous interval of 62 cycles, between the 144th and 206th cycles, when they were in a wet state, as opposed to 36 cycles in other state alternations, as can be seen in Table 3.8.

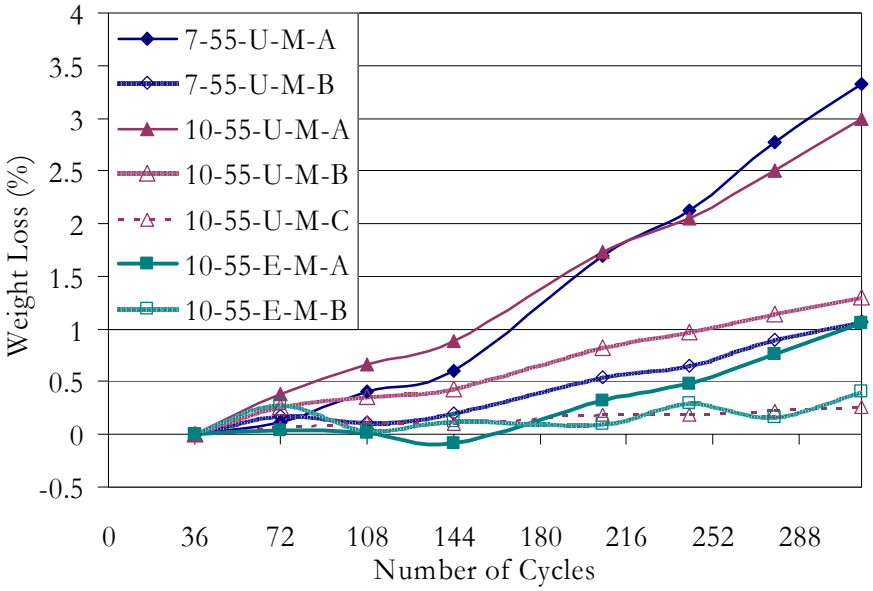


Fig. 3.16: Weight loss in specimens in Series 2

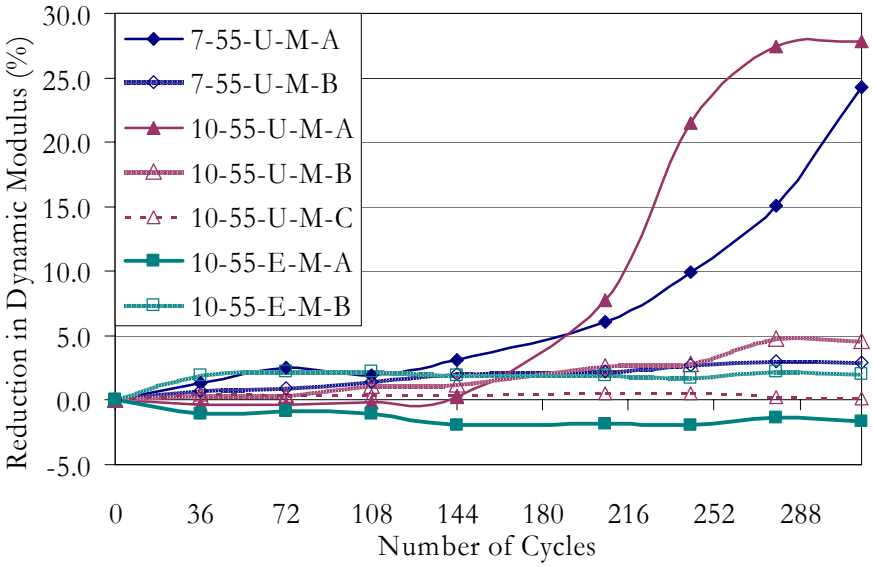


Fig. 3.17: Reduction in Young's dynamic modulus in specimens in Series 2

### 3.2.4 Results

#### *3.2.4.1 Weight Loss and Relative Dynamic Modulus*

The weight losses measured in the specimens have been shown in Fig. 3.16. Like in Series 2, to avoid errors in weight measurement due to excessive water absorption during the initial cycles, the weight loss has been calculated compared to the weights after the 36th cycle. The reduction in the Young's dynamic modulus of the specimens has been shown in Fig. 3.17. It can be seen from these figures that the specimens in wet state throughout the test, and without air-entrainment, viz. 7-65-U-M-A and 10-65-U-M-A, suffered the highest damage. Even though the weight losses for the specimens were only around 3%, reductions in young's dynamic modulus by around 25% were observed. It can thus be concluded that though the scaling in the specimens was low, cracking inside the specimens was considerably higher. It must be noted here that penetration of water into the specimens, as discussed later in Chapter 5, would also lead to reductions in observed weight losses. Little damage was observed in 10-65-U-M-C, which was in dry state throughout. Fig. 3.18 shows the specimens at the end of all freeze-thaw cycles.


Fig. 3.18: Specimens of Series 2 at the end of all Freeze-thaw cycles

#### *3.2.4.2 Strain Variations*

A hysteresis behavior, similar to that in Series 1, was also observed in this series. Residual strains were found to continuously increase for specimens under A-type conditions. However, the residual strains were found to increase during wet cycles

and reduce initially to a constant value during dry cycles for specimens under B-type conditions. The residual strain in specimens under C-type conditions was found to remain almost constant throughout the cycles.

Apparent thermal expansion coefficient ($\alpha_{app}$) for this series was found to depend on the level of deterioration, and thus on mix proportions of the specimens and the exposure conditions. Since, the maximum temperature in this series was lower than in Series 1, $\alpha_{app}$ could be calculated only for temperatures below 0°C. The strain variations in this series of experiments will be discussed further in subsequent chapters.

## 3.3 OTHER SERIES

### 3.3.1 Series 3: Longer cycle time

At the end of Series 2, the three specimens with mold gauges used in Series 1 and the seven specimens with mold gauges from Series 2 were subjected to 5 cycles of 36-hour period with the temperature varying between +20°C and -25°C. All A and B type specimens were kept submerged under water, while the C type specimen was kept dry. It should be noted here that since the specimens from Series 1 were in a dry state before the start of the experiments, all specimens were kept submerged under water for around 10 days before the start of these cycles. The temperature variations at the center of the three specimen sizes and in the thermal exchange fluid are shown in Fig. 3.19. As can be seen from the figure, apart from the region around 0°C, the temperature variation was almost linear. Fig. 3.20 shows the strain-temperature behavior of one specimen of each size for the entire 5 cycles in this series. It should be noted that in this figure, zero-strain has been set so as to prevent overlapping of the three curves. Due to a low temperature rate, the thermal gradients within the specimens were also found to be lower and the strain-temperature behavior was almost linear. $\alpha_{app}$ can be easily calculated individually during freezing and thawing during this series due to the near-linear behavior observed.

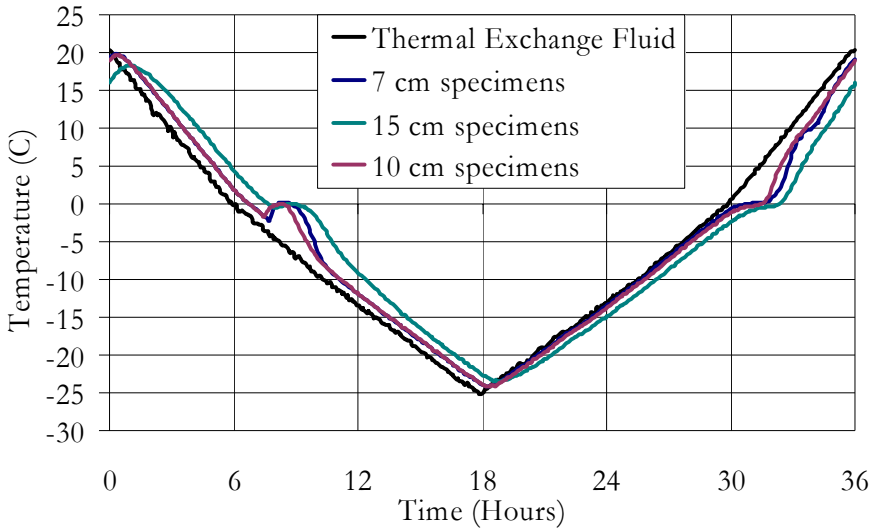


Fig. 3.19: Temperature variations during 36-hour cycles

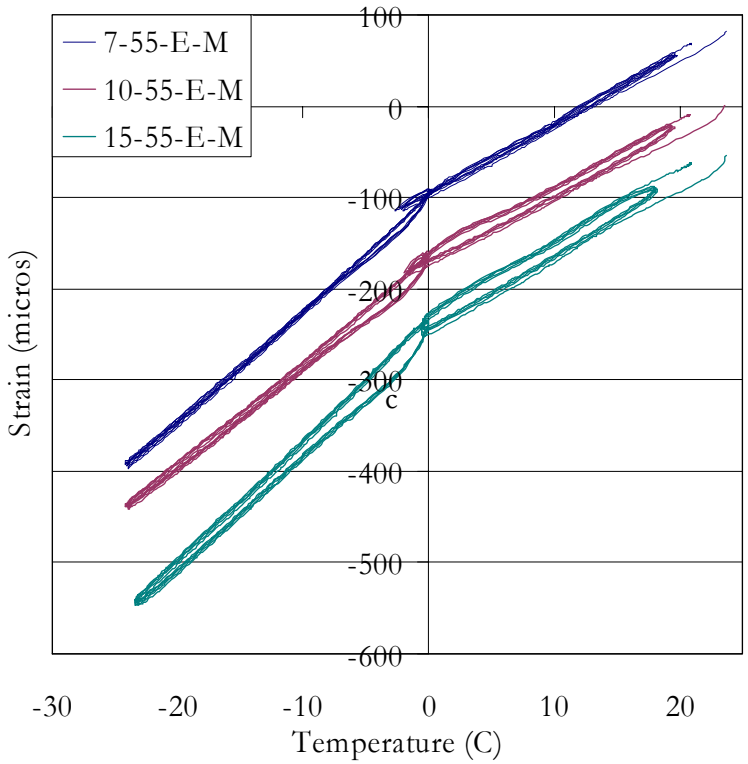


Fig. 3.20: Strain-Temperature variations during 36-hour cycles

### 3.3.2 Series 4: Test for $\alpha_{app}$ over 0˚C

Since $\alpha_{app}$ could not be measured for temperatures over 0˚C in Series 2, 15 cycles, with conditions similar to that used in Series 1, were carried out on the 10 specimens used in Series 3. This series, which was started just after the end of Series 3, has also been used for comparison with Series 3 considering that the specimen conditions would be almost the same in Series 3 and 4.

### 3.3.3 Series 5: Specimens with cracks

This series was carried out alongside Series 2 and has been used only for visual observation. A single crack near the center was induced in each of the reinforced concrete specimens using three point flexural loading. Fig. 3.21 shows a crack in one of the specimens before any freeze-thaw cycles were carried out. Details of the specimens are given in Table 3.9 along with the crack width before the start of the freeze-thaw cycles. The concrete mix and specimen coding of the specimens in this series is same as in Series 2. The 'X' in the specimen code denotes presence of crack in the specimen. The specimens were reinforced with a high yield smooth steel bar with a 13 mm diameter at the center. The steel bar was 38 cm long with 1 cm of the bar protruding from both ends of the specimen. Though the observations from this series of experiments shall be discussed here, the relevance of this series of experiments shall be explained later in Chapter 5.

Table 3.9: Details of specimens in Series 5

| S.No. | Specimen code | Mix no. | Size (cm) | Crack width (mm) | No. of cycles | Exposure condition |
|---|---|---|---|---|---|---|
| 1 | 7-65-U-X-A | M-65-U | 7x7x36 | 0.15 | 206 | Wet throughout |
| 2 | 7-65-U-X-B | | | 0.35 | 314 | Alternating wet and dry |
| 3 | 10-65-U-X-A | | 10x10x36 | 0.4 | 72 | Wet throughout |
| 4 | 10-65-U-X-B | | | 0.3 | 36 | Alternating wet and dry |
| 5 | 10-65-U-X-C | | | 0.45 | 314 | Dry throughout |
| 6 | 7-65-E-X-A | M-65-E | 10x10x36 | 0.25 | 314 | Wet throughout |
| 7 | 10-65-E-X-A | | | 0.45 | 314 | Wet throughout |
| 8 | 10-65-E-X-B | | | 0.3 | 314 | Alternating wet and dry |
| 9 | 10-65-E-X-C | | | 0.5 | 314 | Dry throughout |

The specimens were placed alongside specimens in Series 2 and were thus subjected to same conditions as in Series 2. Fig. 3.22 shows the specimens at the end of the freeze-thaw cycles. It can be seen from these pictures that the damage was extremely accentuated in specimens without entrained-air and submerged in water, in which the crack widths were found to increase to as much as 1 cm in width. This can be clearly contrasted with the dry specimens and air-entrained specimens, where no such accentuated crack widening was observed. Table 3.9 also lists the number of freeze-thaw cycles each specimen was subjected. As can

be seen from the table, freeze-thaw tests on some specimens were discontinued after the crack was wide enough and passed through the entire width of the specimen.

Fig. 3.21: Crack in specimen before subjecting to freeze-thaw cycles


Fig. 3.22: Cracked specimens after freeze-thaw deterioration

The cracks in both 10 cm size specimens without air-entrainment submerged under water were found to widen excessively within the first 72 cycles (36 cycles in one case), whereas no such widening was observed in dry and air-entrained

specimens even at the end of 314 cycles. The widening was relatively slower in 7-65-U-X-A, with the process being more gradual and progressive when compared to the sudden widening observed in larger specimens. It can be also seen in 7-65-U-X-B that the widening is lower compared to the 10 cm specimens even at the end of 314 cycles, of which a total of 170 cycles were wet. The widening was again found to be much lower in the case of the smaller entrained specimen. A further discussion of these observations and their relevance to the current discussion shall be discussed later in Chapter 5.

# Chapter 4

# DISCUSSION OF RESULTS

A brief overview of the results from the experiments was presented in Chapter 3. In this chapter, results directly pertinent to this study shall be presented in greater detail and a discussion of the implications of the observed results shall follow. Results from all series of experiments have been presented and compared in this chapter and it has been assumed that no differences in experimental conditions other than those mentioned earlier exist.

## 4.1 STRAIN-TEMPERATURE VARIATION

### 4.1.1 Analytical verification of strains

Before analyzing the strain-temperature behavior further, it is important to verify the trend of the results with calculated values in order to present a convincing argument. Most of analytical methods that can be used to evaluate strains make inherent assumptions as to the elastic nature of the material. Residual strains and effect of damage, thus, being difficult to calculate; only the effect of thermal gradients on strain variations shall be analyzed here in order to verify the experimental results and the assumption that thermal-gradients are the main cause of the observed hysteresis.

Firstly, a relation between temperature and strain at the center of the specimen shall be derived based on various assumptions and simplifications and it shall then be compared to results from a Finite Element Analysis (FEM). FEM is a widely used tool used for accurate analysis of many different materials. Though this

analysis is currently not very accurate for concrete-like materials, for the sake of comparison, it shall be considered here that the analyzed concrete is elastic in nature, and has no cracks. Thus, in case of a close agreement between FEM analysis and the derived relations, the relation shall be considered acceptable for the purpose of verification of the trend of the results. This is being done since FEM analysis involves long modeling and analysis times. However, such a derivation can enable quick estimations of approximate strains using simple spreadsheet applications.

#### *4.1.1.1 Derivation of strain dependence on temperature*

In order to estimate the strain at the center of a prismatic specimen with a square cross-section, we shall first characterize the temperature distribution in the body of the specimen in terms of the temperature at the center and the surface. If the temperature (T) in a body changes both with time (t) and location (x, y and z, in Cartesian coordinate system), the heat transfer in the absence of a heat source inside is characterized by the well known heat equation shown in Eq. 4.1.

$$\frac{\partial T}{\partial t} = D \cdot \left( \frac{\partial^2 T}{\partial x^2} + \frac{\partial^2 T}{\partial y^2} + \frac{\partial^2 T}{\partial z^2} \right) \tag{4.1}$$

Where, D is the thermal diffusivity of concrete, calculated to be $7.27 \times 10^{-7}$ m²/sec in §3.1.4.2.

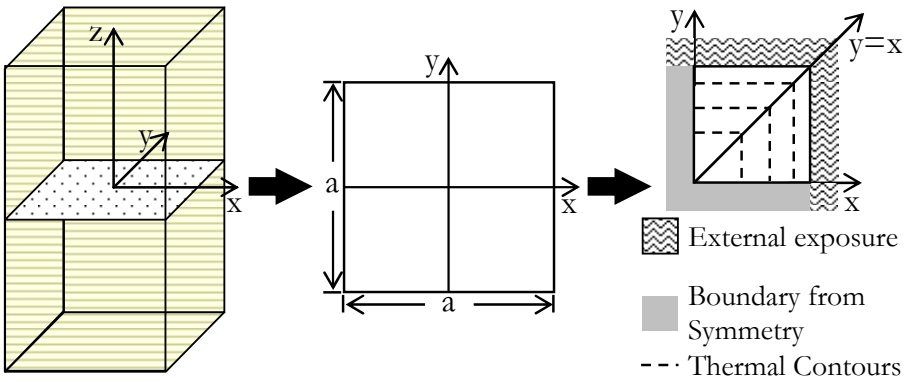


Fig. 4.1: Simplifications in analytical thermal calculations

It can be safely assumed that the temperature is uniform along the z axis in the vicinity of the plane *z=0,* due to the z-dimension of the specimens being much larger than the x and y dimensions, as shown in Fig. 4.1. In other words:

$$\left|\frac{\partial^2 T}{\partial z^2} = 0\right|_{z=0} \tag{4.2}$$

The three-dimensional problem characterized in Eq. 4.1 would thus be reduced to two-dimensions. We further assume the temperature to be constant throughout the surface of the specimen and a perfect symmetry about the x and y axes. Assuming the thermal contours to be running parallel to the surface of the specimen and considering the temperature variation only along the line $x=y$, the problem can be further reduced to only a single dimension as below.

$$\left|\frac{\partial^2 T}{\partial x^2} = \frac{\partial^2 T}{\partial y^2}\right|_{y=x} \tag{4.3}$$

Thus,
$$\frac{\partial T}{\partial t} = 2D \cdot \frac{\partial^2 T}{\partial x^2} \tag{4.4}$$

We further assume that the rate of change of temperature linearly varies with x, thus:

$$\frac{\partial^2 T}{\partial x \partial t} = \text{constant} \tag{4.5}$$

Assuming the rate of temperature on the surface to be $K_0$(t) and that at the center of the specimen $K_i$(t), Eq. 4.4 can be rewritten as:

$$K_i + \frac{(K_0 - K_i)}{a} \cdot 2x = 2D \cdot \frac{\partial^2 T}{\partial x^2} \tag{4.6}$$

Where $a$ is the length of the side of the square cross-section of the specimen. Since the temperature at the surface ($T_0$(t)) and at the center ($T_i$(t)) is known, Eq. 4.6 can be integrated twice with the application of the boundary conditions to obtain:

$$T = \frac{K_i}{4D}x^2 + \frac{(K_0 - K_i)}{6aD}x^3 + \left(\frac{2(T_0 - T_i)}{a} - \frac{K_0 + 2K_i}{24D}a\right) \cdot x + T_i \tag{4.7}$$

Eq. 4.7, thus, gives the temperature distribution on the line as a function of temperatures and temperature rates on the surface and at the center. Since these values are known from the experiments, the approximate thermal gradients can hence be estimated.

In order to calculate the approximate strains from these thermal gradients, we shall assume that the strain within the specimen is uniform throughout the *xy* plane for a given moment in time. Though this assumption would hold for smaller specimens, as used in this study, they would not be appropriate for larger specimens, where plane deformations are not negligible when compared to the overall deformations. The plane for which the thermal gradients have been calculated above can thus be modeled as a system of parallel elastic springs with equal natural lengths ($l_0$) at a base temperature of $T_b$ and equal deflection ($\Delta l$) at any moment in time. This setup is illustrated in Fig. 4.2.

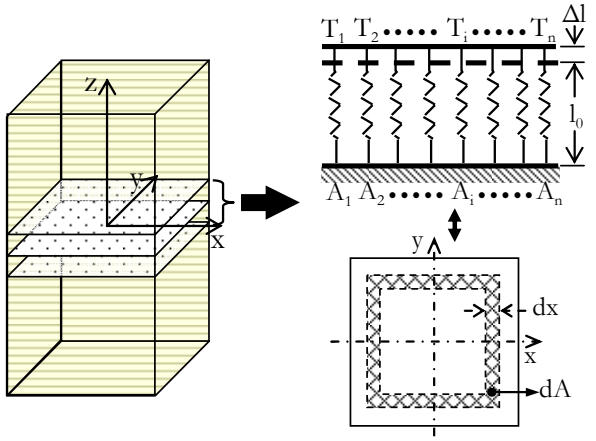


Fig. 4.2: Simplified modeling for strain calculations

Here, a small region around the plane *z=0* would be considered composed of infinite concentric hollow pipes of square cross-section with cross-section area $dA_i$ and uniform temperatures throughout each pipe. If each pipe is considered as an individual independent spring, the length of the spring at a temperature T would be:

$$l_T = l_0\left(1+\alpha\left(T-T_b\right)\right) \tag{4.8}$$

Where α denotes the thermal expansion coefficient of the material of the springs and is uniform for all springs. However, since each spring is restrained by the

other springs, which have a different temperature, all springs have an equal length of $l_0+\Delta l$. The summation of forces in individual springs can thus be equated to zero since the system is in equilibrium.

$$\sum_i F_i = \sum_i E \cdot dA_i \cdot \left(l_0 + \Delta l - l_0\left(1+\alpha\left(T_i - T_b\right)\right)\right) = 0 \tag{4.9}$$

For the sake of simplicity we can assume $T_b$ to be 0. Here the strain (ε) can be defined as $\frac{\Delta l}{l_0}$. Eq. 4.9 can thus be rewritten as:

$$\sum_i dA_i\left(\varepsilon - \alpha T_i\right) = 0 \Rightarrow \sum_i dA_i \varepsilon = \sum_i dA_i \alpha T_i \Rightarrow \varepsilon = \alpha \cdot \frac{\sum_i T_i \cdot dA_i}{A} \tag{4.10}$$

Where A is the total cross section area of the specimen and equals $a^2$. Considering such infinite elements in the specimen, and replacing dA by *8x ∂dx*, Eq. 4.10 can be rewritten in the integral form as below.

$$\varepsilon = \frac{8\alpha}{A}\int_0^{a/2} Tx\,dx \tag{4.11}$$

Eq. 4.7 can be substituted in Eq. 4.11 and solved to calculate ε as below.

$$\varepsilon = \frac{8\alpha}{A}\left(\frac{K_i}{256D}a^4 + \frac{K_0 - K_i}{960D}a^4 + \frac{T_i}{8}a^2 + \frac{b}{24}a^3\right) \tag{4.12}$$

Where,

$$b = \frac{2}{a}\left(T_0 - T_i - \frac{K_0 + 2K_i}{48D}a^2\right) \tag{4.13}$$

Using the above calculated relations, an approximate value of the strains can be calculated based only on temperature variations on the surface and the center of the specimens. $K_0$ and $K_i$ can be calculated in various ways if the temperature variations with time are known. The strength of this method lies in obtaining quick solutions for different specimens and even upon changing material parameters for the same specimen, which would normally require repetition of the entire analysis if FEM analysis is used.

#### *4.1.1.2 Verification of derived relation*

The above derived Eqs. 4.12 and 4.13 have been compared to a solution obtained using a high resolution FEM analysis and have been shown in Fig. 4.3. The analysis was carried out using the software Ansys 6.0. The same material

parameters were input in both case and the temperature variations were close to those observed in actual experiments. Though the agreement between the two curves is not exact, it can still be seen that a close and acceptable trend of strain-temperature variations can be obtained using the above formulated relations. The formulation would thus be considered acceptable and will be used for verification of experimental results.

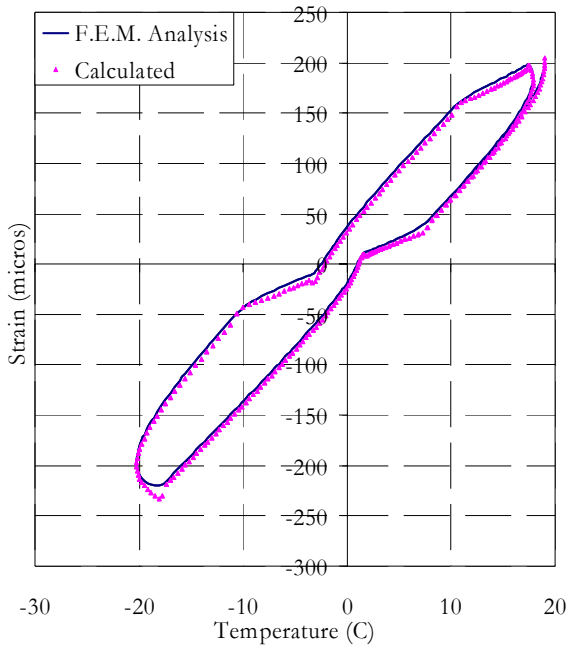


Fig. 4.3: Comparison of calculated strains with FEM analysis

#### *4.1.1.3 Comparison of experimental and calculated strains*

The experimentally obtained strains for a few cycles were compared with calculated values neglecting residual strains. A good agreement was found between the experimental and calculated values in most cases, allowing for the assumptions made during the derivation of the analytical equations. However, this agreement could only be obtained either above 0°C or below 0°C at a time for every specimen. This is because, as mentioned before, the apparent thermal expansion coefficient of the specimens was higher below 0°C than above 0°C. So, the results have been individually compared for both ranges of temperatures. Some of the compared results are presented in Fig. 4.4.

The experimental results can thus be considered to be accurate in nature and it can be concluded that most of the hysteresis observed in the strain-temperature

relationship is due to temperature gradients. It can also be conclusively said from this comparison that $\alpha_{app}$ is comparatively higher below 0°C.

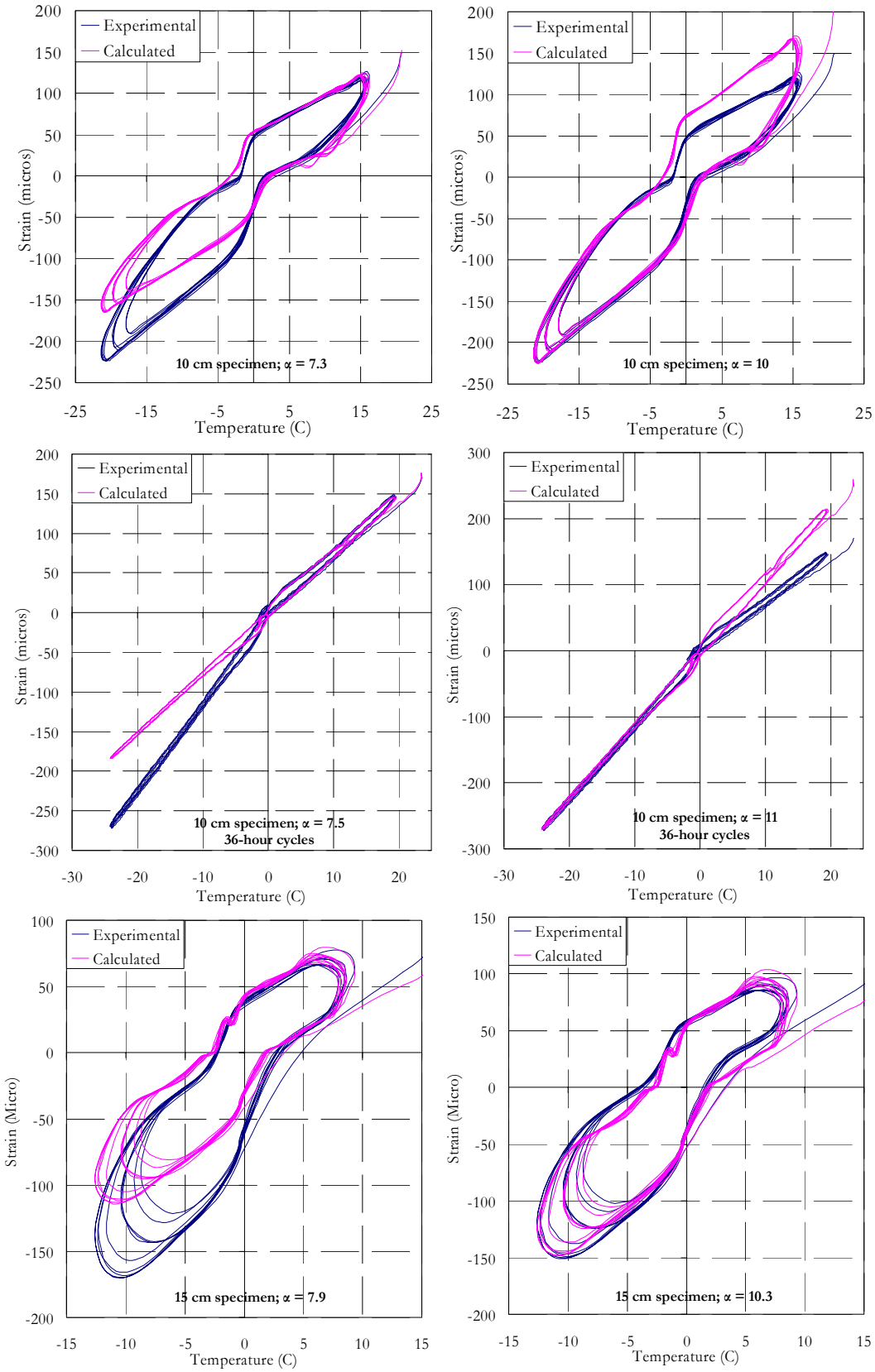


Fig. 4.4: Comparison of experimental results with calculated values

### 4.1.2 Anomalies in Strain-Temperature Curves

It was seen in Chapter 3, that in Series 1, the shape of strain-temperature curves remained almost the same and predictable throughout the freeze-thaw cycles since the damage was small. It has also been shown above that despite an apparent increase in thermal expansion coefficient below 0˚C strain variations roughly follow a linear elastic variation. However, it was observed that the strain-temperature variation changes as deterioration progresses in a specimen. Figs. 4.5 to 4.7 show the strain temperature variation of Series 2 specimens during the 5th and 313th cycles for A and C-type exposure specimens, and 5th and 277th cycles for B-type exposure specimens. It should be noted here that in these curves, the zero-strain value for each specimen has been set at different values so as to avoid overlap of curves.

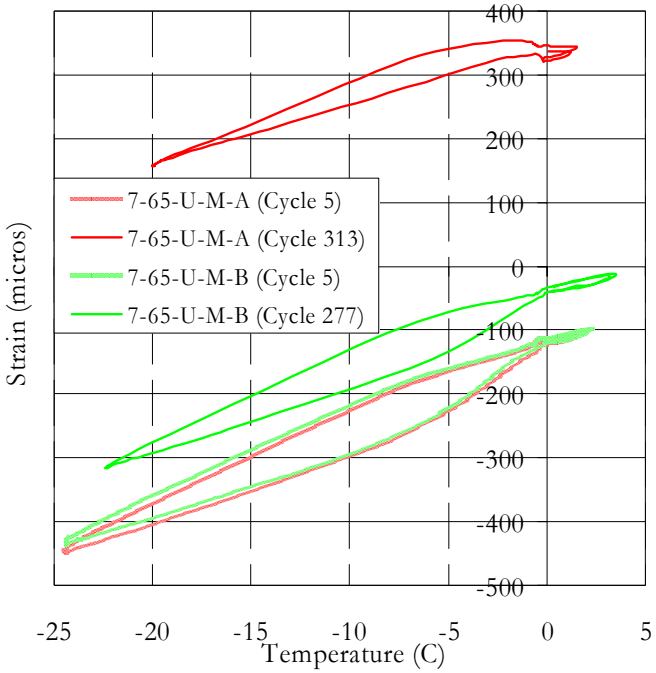


Fig. 4.5: Strain-temperature curves for un-entrained 7 cm specimens

A large change in the strain-temperature behavior for specimen 10-65-E-M-A was noticed starting around 150th cycle even though little damage was observed on the specimen. This change is thus probably because of localized changes around the strain gauge, rather than the entire specimen. In this strain gauge, an abrupt reduction in strain was observed near 0˚C. Collection of water at the surface of the strain-gauge is thus believed to be the reason for this behavior. The expansion

and contraction of water upon freezing and thawing, respectively, at the surface of the strain gauge would induce sudden and complex contractions and expansions in the strain gauge thus causing erroneous measurements around 0˚C. Residual strains for Series 2 specimens have thus been calculated at a temperature of -15˚C in order to avoid errors discussed above.

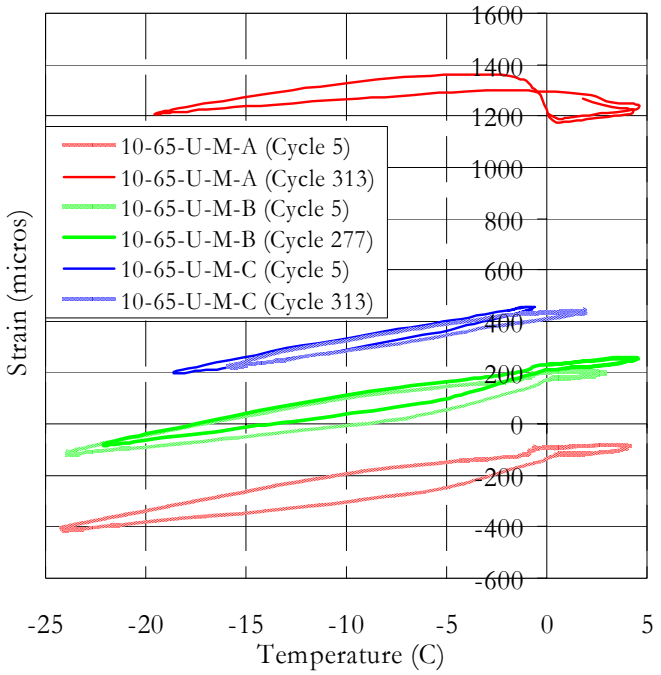


Fig. 4.6: Strain-temperature curves for un-entrained 10 cm specimens

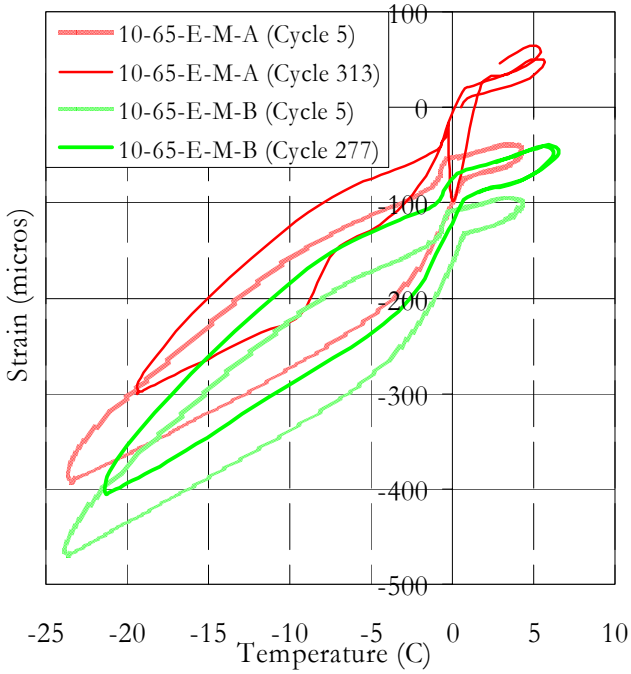


Fig. 4.7: Strain-temperature curves for air-entrained 10 cm specimens

Apart from the observation discussed above, it was observed that the shape of the strain-temperature variation does not change much during the tests for the specimens that showed smaller damages. However, an increase in strain just below 0°C, signifying expansion, was noticed in specimens with higher damage. Also, a contraction while thawing, around the same temperatures, was noticed for these specimens. However, it was observed that the entire expansions were not reversible and the strains were found to increase in progressive cycles.

Freeze-thaw damage is usually in the form of cracking inside concrete. In cases of severe deteriorations, the cracks would expand to sizes larger than the pore-sizes and would be filled by water if available. Due to the large size of these cracks, this water would freeze at temperatures close to 0°C and would cause expansion in the concrete and also widen the cracks. Only a part of this expansion would be reversible upon release of tensile pressure due to thawing, while the irreversible expansion would be filled by water, if available, and this process would continue. Monitoring of strain-temperature behavior can hence provide useful information regarding the health of the specimen and growth of cracks.

## 4.2 RESIDUAL STRAINS

Residual strains are here defined as the change in strain of the specimen with the progress of cycles, when measured at the same temperature. As mentioned earlier, residual strains were generally found to increase with the progress of deterioration of specimens. The observed variations of residual strains from the experiments described earlier will be discussed in this section.

### 4.2.1 Importance of Residual Strains

The measurement of residual strains here is analogous to the measurement of change in length of specimens that has historically been used as a measure of freeze-thaw deterioration. However, measurement of residual strains may have certain inherent advantages when compared to other evaluation methods, such as,

- Residual strains can be measured for each cycle at any desirable temperature, without having to disturb the testing process,
- Scaling, which is known to progress independent of cracking, and is mostly a surface phenomenon would create inaccuracies in measurements, however, since residual strains can be measured in a comparatively smaller region inside concrete, it can be ensured that the measured region has no scaling,
- Strain-data is usually electronic in nature and can easily be recorded and monitored remotely without any manual intervention, and
- Residual strain measurements would generally be more accurate and continuous when compared to other manually recorded measurements.

Thus, the quantification of damage in concrete in terms of residual strains would be advantageous for monitoring structural health. Also, as will be discussed later, not only residual strains, but also other parameters related to strain-temperature behavior of concrete can be used to evaluate and even predict the performance of concrete.

The experimental results obtained show the dependence of residual strains on various factors, and specially saturation level of concrete. In normal conditions, physical loads, which have not been investigated in this study, would also play a large role in the variation of residual strains. It is thus important to study the effect of various factors on residual strains in order to be able to effectively use them for damage evaluation.

### 4.2.2 Slight Deteriorations

Fig. 4.8 shows the residual strains in specimens of Series 1 measured at 20°C. The relatively large increase during the first 36 cycles can be attributed to saturation of specimens as discussed earlier in §3.1.3.2. However, even after the apparent saturation of specimens, the residual strains are seen to rise with the progress of cycles. It was seen in §3.14 that the damage in these three specimens was small

and could not be effectively measured using conventional test methods. The continuous monotonic rise of residual strains during the wet cycles shows that residual strains can be used to measure even small damages in concrete, which might otherwise go undetected.

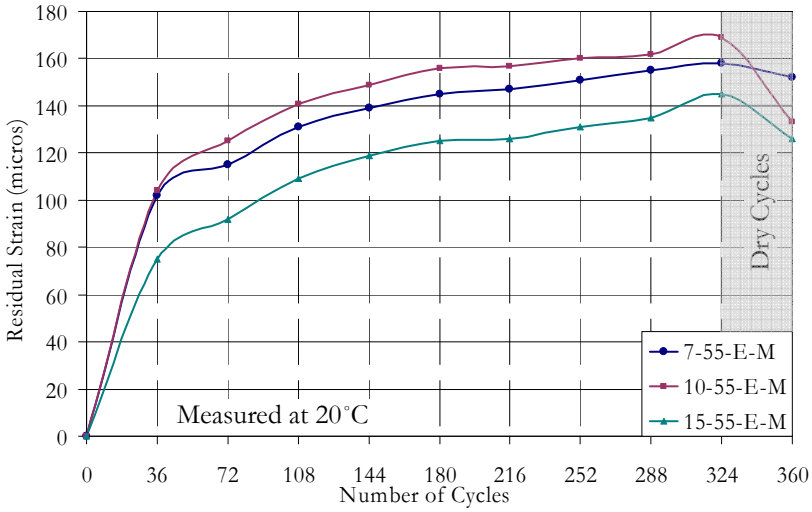


Fig. 4.8: Residual strains in specimens in Series 1

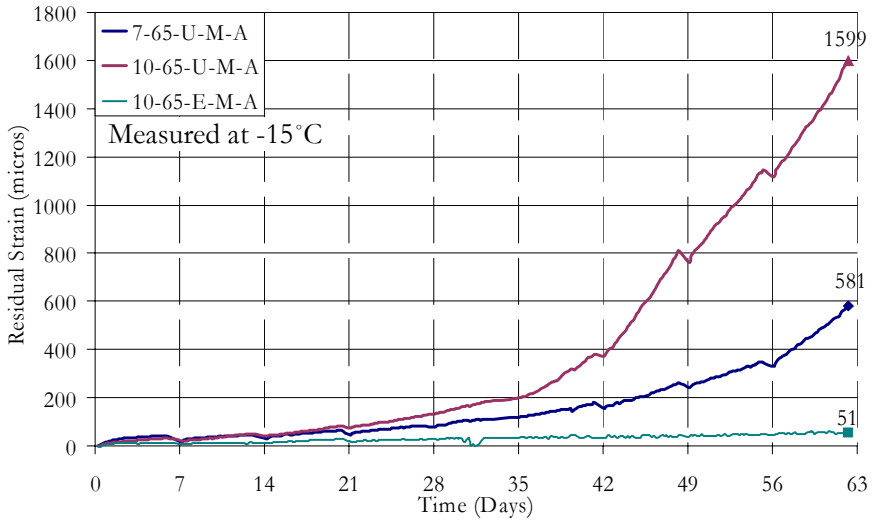


Fig. 4.9: Residual strains for specimens in wet state throughout in Series 2

### 4.2.3 Severe Deteriorations

Residual strains were found to increase progressively in specimens under wet state throughout the test as shown in Fig. 4.9. These residual strains were measured at -15˚C in order to avoid errors due to abrupt transient changes near 0˚C discussed earlier in this chapter. The equivalent number of cycles for the number of days has been listed earlier in Table 3.8. Residual strain was found to reach over 1500μ in the specimen 10-65-U-M-A and over 500μ in the specimen 7-65-U-M-A.

This increase is extremely high when compared to the specimen 10-65-E-M-A, which, though under similar conditions, had entrained air, and had a final residual strain of only around 50μ. These results can be seen to be consistent with the increase in weight loss and the reduction in Young's dynamic modulus shown earlier in Figs. 3.16 and 3.17.

A slight reduction in residual strains was observed after every 36 cycles due to the drying of specimens during weight and dynamic modulus measurements. Neglecting this reduction due to change in conditions, it can be seen that residual strains rise monotonically throughout the test. The rate of damage can also be observed to increase with the progress of cycles. External conditions remaining the same, progressive deterioration can thus be monitored using residual strains. The effects of various external factors shall be discussed in the subsequent sections.

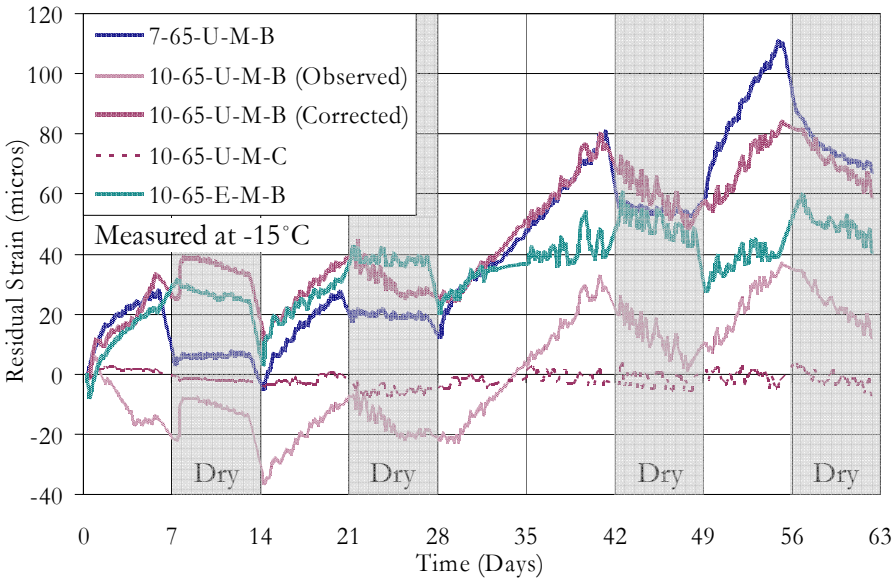


Fig. 4.10: Residual strains for specimens with dry cycles for Series 2 at -15°C

### 4.2.4 Effect of Degree of Saturation

Fig. 4.8 also shows a reduction in strains during the dry cycles in Series 1. Drying is known to cause shrinkage in concrete. Loss of moisture from concrete would thus lead to reduction in residual strains, other factors remaining the same. Further, since moisture is an important factor affecting freeze-thaw deterioration, the growth of residual strains would be curbed. Dry cycles can, thus, lead to a

reduction in residual strains within concrete. Influence of dry cycles on different specimens as observed in Series 2 has been shown in Fig. 4.10.

Little changes in residual strains with the progress of freeze-thaw cycles were found to occur in the specimen 10-65-U-M-C, which was in a dry state throughout the test. In this specimen, there was a slight increase in the residual strains during the initial few cycles possibly due to a small damage in the specimen since it had a high saturation before the start of cycles. This was followed by a small reduction in the residual strains, possibly due to drying of the specimen. Strains after that remained almost the same throughout the test. As shown in §3.2.4.1 earlier, almost no damage was observed in this specimen even at the end of the freeze-thaw cycles.

The strains in specimen 10-65-U-M-B during the initial 36 cycles were found to be inconsistent with the other results probably due to experimental errors. Since the conditions of this specimen were the same as specimen 10-65-U-M-A up to 36 cycles, for comparison purposes, the residual strains in the specimen 10-65-U-M-B were corrected such that the value at the end of 36 cycles was the same as that for the specimen 10-65-U-M-A.

Strains were found to increase during the wet cycles in the specimens subjected to alternating wet and dry cycles. B-type specimens were subjected to a total of 170 wet cycles, equivalent to 35 days of wet cycles in specimens in wet condition throughout. The residual strains in B-type specimens at the end of 170 wet cycles are close to those observed for A-type specimens at 35 days, except for the specimen 10-65-U-M-B where the residual strains were around half those observed in 10-65-U-M-A. The highest gain in residual strain in all specimens was found to occur between the 28th and 42nd days when the specimens were subjected to 62 continuous wet cycles.

It is apparent from the above discussion that almost no damage occurs during dry cycles. Intermittent dry cycles also lead to removal of water from the specimens,

which can slow down the freeze-thaw process. It also follows logically that ingress of water into the specimens also significantly contributes to increasing apparent residual strains along with cracking of concrete. Removal of water would similarly lead to a reduction in residual strains due to drying shrinkage. This would also cause closing of some of the cracks generated by freeze-thaw deterioration, thus further reducing the residual strains.

Reduction of residual strains, thus, does not necessarily denote lesser damage. Most of the damage caused during cyclic freezing and thawing is irreversible in nature and thus the last peak level of residual strains should be considered for estimating damage in the concrete.

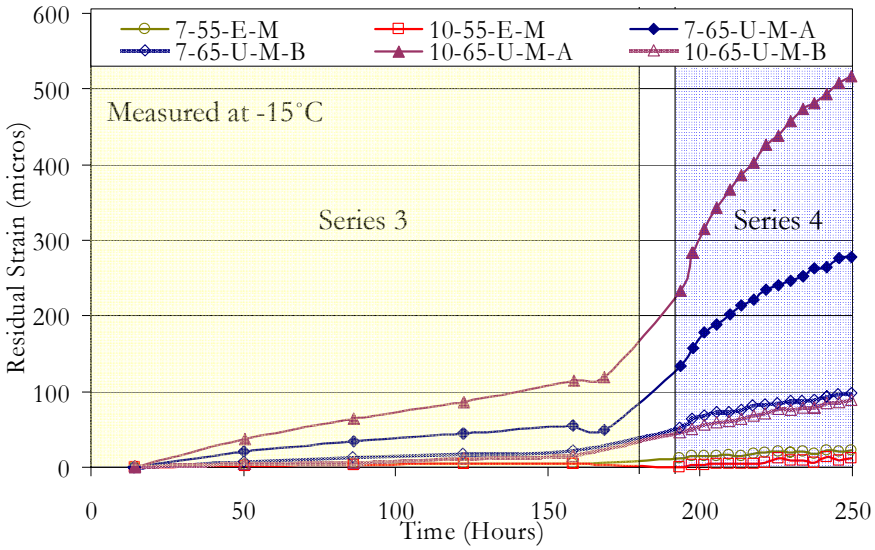


Fig. 4.11: Residual strains for Series 4 and 5 at -15°C

Fig. 4.11 shows the increase of residual strains during Series 3 and 4 for specimens with significant strain increase. It can be seen deterioration continued at a high rate in specimens without air-entrainment that were subjected to A-type conditions in Series 2. Also, the deterioration rate was high in similar specimens that were under B-type conditions in Series 2, but were placed under water in Series 3 and 4. The per-hour damage appears to be higher during the 4-hour cycles when compared to the 36-hour cycles, when the specimens were also subjected to a larger number of cycles in the same amount of time. However, given the limited number of cycles in these series, it is difficult to draw further conclusions from these results.

## 4.3 APPARENT THERMAL EXPANSION COEFFICIENT

As mentioned earlier, the apparent thermal expansion coefficient ($\alpha_{app}$) of specimens was observed to be higher below 0˚C than above it. Average $\alpha_{app}$ for each cycle was calculated using linear regression to remove the effect of hysteresis from strain-temperature curves. The slopes above 0˚C were calculated for points with temperature above 4˚C and below 0˚C for temperatures below -4˚C. This was done in order to avoid noise due to transient effects around 0˚C as discussed in §4.1.2. $\alpha_{app}$ above and below 0˚C for Series 1 have been plotted in Fig. 4.12. Due to the short temperature range and large hysteresis, accurate estimates of $\alpha_{app}$ for 15 cm specimen could not be obtained. Though the values are quite scattered, it can be seen that no large variations in $\alpha_{app}$ exist in the specimens in Series 1. $\alpha_{app}$ was, however, found to vary with moisture and level of deterioration in specimens in Series 2. Values of $\alpha_{app}$ during individual freeze-thaw cycles and 36 cycle moving averages are shown in Figs. 4.13 to 4.15. The moving averages, representing the overall trend of the values, would be easier to understand since various experimental factors would increase the scatter of values for individual cycles.

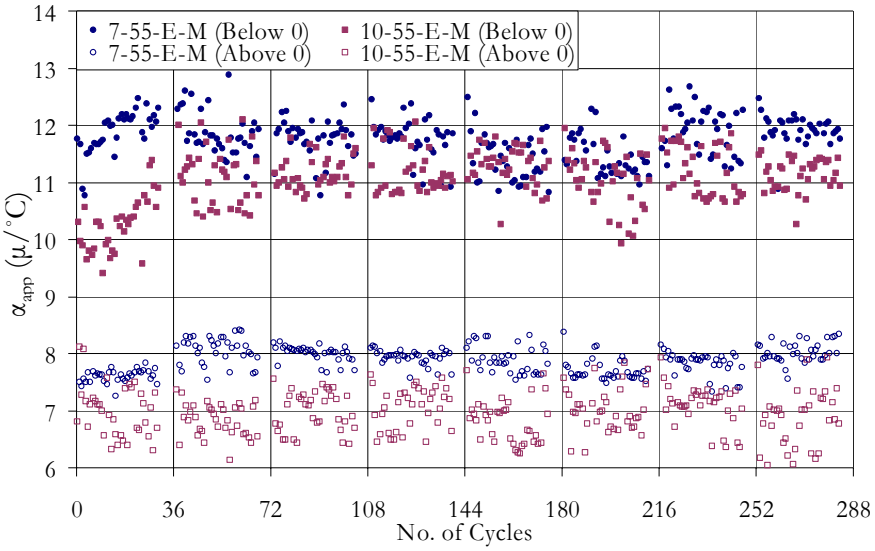


Fig. 4.12: Apparent thermal expansion coefficients during Series 1

It can be seen from figure Fig. 4.13 that $\alpha_{app}$ reduces with time in case of severe deteriorations. By comparison with residual strains, it is observed that reduction in

$\alpha_{app}$ increases the rate of increase of residual strains. However, even if $\alpha_{app}$ ceases to reduce after some transient reduction, as can be seen in specimen 10-65-U-M-A between 49th and 63rd days, residual strain continues to rise. Measurement of $\alpha_{app}$ can thus be used to monitor the vulnerability of the specimen. Observed reductions in $\alpha_{app}$ would indicate that any further freeze-thaw cycles on the specimen would cause severe damage at increasing rates.

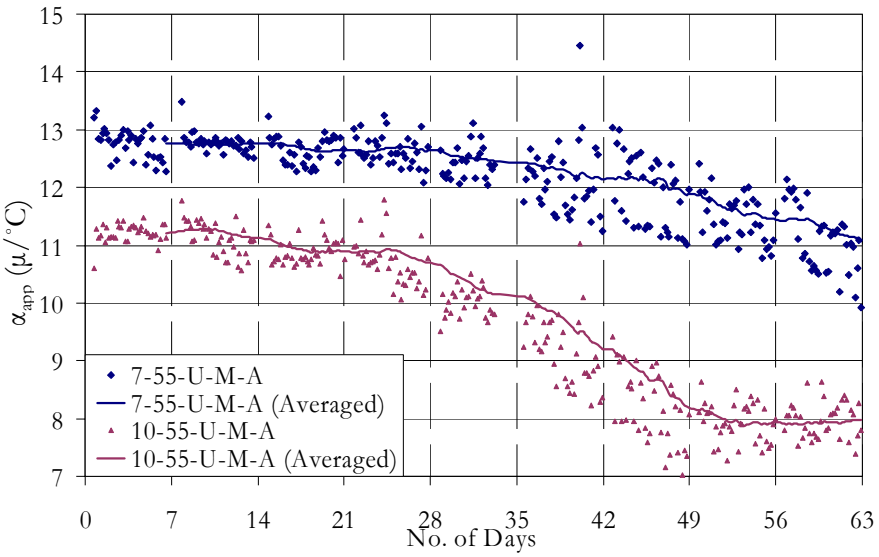


Fig. 4.13: Apparent thermal expansion coefficients for specimens with severe deterioration

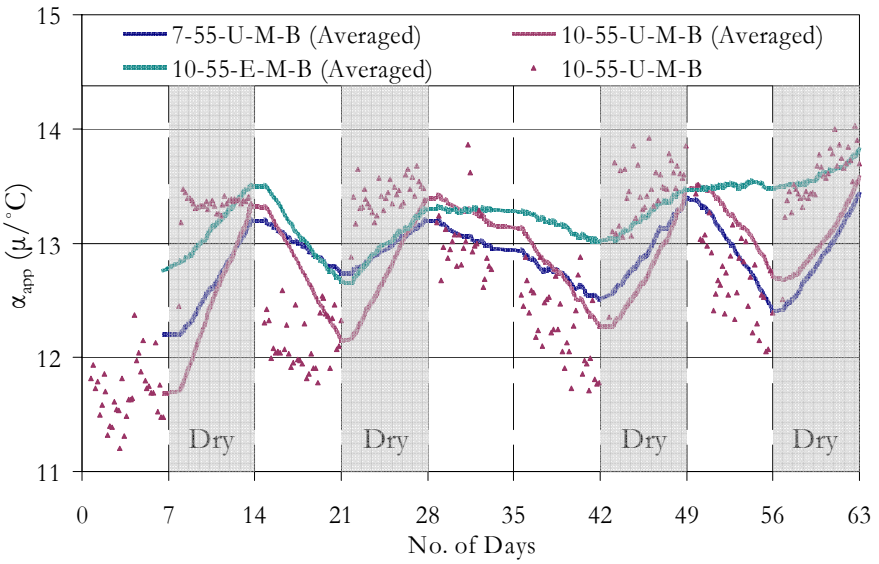


Fig. 4.14: Apparent thermal expansion coefficients for B-type conditions

Specimens under B-type conditions were observed to have a higher $\alpha_{app}$ during dry cycles when compared to the wet cycles, as can be seen in Fig. 4.14. Though

this trend continued in the un-entrained specimens, the difference in $\alpha_{app}$ between wet and dry cycles was observed to reduce with the progress of cycles.

It was also observed that $\alpha_{app}$ was higher for the specimen in dry state throughout (Fig. 4.15). The value, though observed to reduce initially and remain constant through the later cycles, was still higher than that observed in other specimens. The scatter in the values was also observed to be lower with the values being closer to the average than other specimens probably due to the continuously consistent experimental conditions the specimen was subjected to. Interpretation of the variation observed in the specimen 10-65-E-M-A was difficult since the values were highly dispersed after the initiation of the anomaly near 0˚C discussed in §4.1.2 However, it could clearly be observed that $\alpha_{app}$ was higher in specimens with air-entrainment.

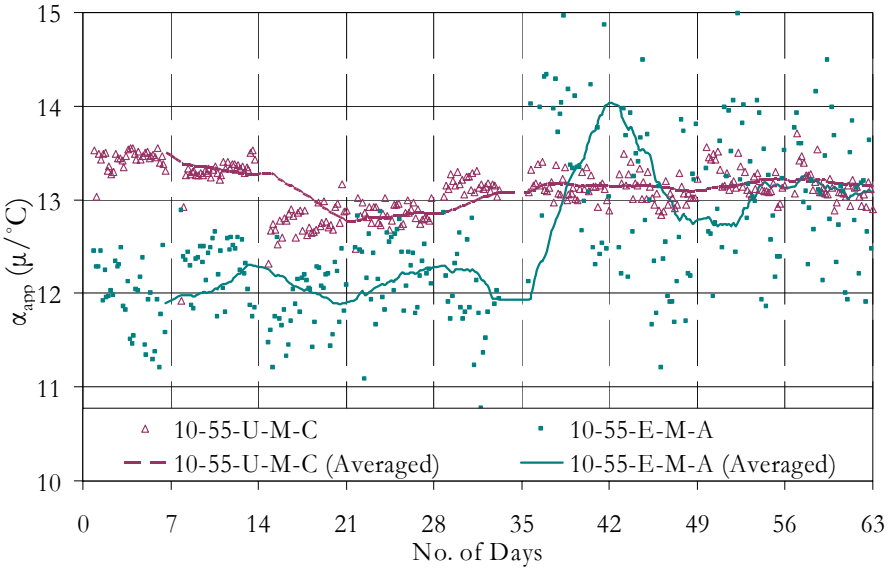


Fig. 4.15: Apparent thermal expansion coefficients in Series 2

Values of $\alpha_{app}$ were calculated and averaged for the entire 5 cycles in Series 3 and 15 cycles in Series 4 and have been shown in Fig. 4.16. Since the strain-temperature behavior was almost linear during Series 3, where the cycle time was 36 hours, separate values could be calculated both above and below 0˚C individually during the freezing and thawing phases. Since Series 4 was carried out continuously after Series 3, the values of the two series can be directly compared. It can be observed that $\alpha_{app}$ below 0˚C is higher during thawing when compared

to freezing for almost all specimens. This difference is, however, smaller in air-entrained specimens when compared to un-entrained specimens. $\alpha_{app}$ was also observed to be higher during 36 hour cycles (Series 3), when compared to 4 hour cycles (Series 4).

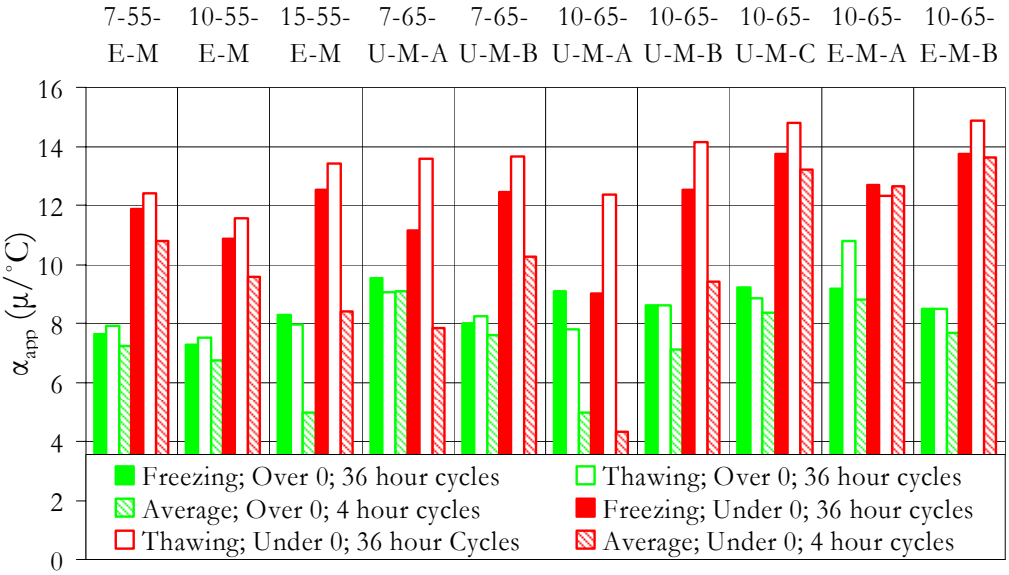


Fig. 4.16: Average apparent thermal expansion coefficients in Series 3 and 4

These observed variations, though macroscopic in nature, can provide us with a better understanding of the microscopic processes during cyclic freeze-thaw deterioration. The causes and consequences of the above described variations in the apparent thermal expansion coefficient shall be further discussed in subsequent chapters.

# Chapter 5

# THE PROCESS OF FREEZE-THAW DETERIORATION

## 5.1 MECHANISMS LEADING TO OBSERVATIONS

### 5.1.1 Main Experimental Observations

Observations from various experiments conducted have been presented and discussed in previous chapters. To the best of the knowledge of the author, such data related to strain variations and apparent thermal expansion coefficients under different moisture conditions during cyclic freezing and thawing has not been presented in earlier studies. The main observations from the experiments have been summarized below.

- Residual-strains increase with deterioration.
- The apparent thermal expansion coefficient ($\alpha_{app}$) has a comparatively higher value under 0˚C than above.
- $\alpha_{app}$ is higher during dry cycles.
- $\alpha_{app}$ is higher during slower cycles.
- $\alpha_{app}$ reduces as deterioration occurs.
- Damage rate increases with the reduction of $\alpha_{app}$.
- $\alpha_{app}$ can reduce to a constant value even if deterioration continues.
- $\alpha_{app}$ is comparatively higher during thawing than freezing in slow cycles.
- Residual strains are lower and $\alpha_{app}$ higher in smaller specimens
- $\alpha_{app}$ is higher in air-entrained concrete.

- In air-entrained specimens under alternating wet and dry conditions, though, initially $\alpha_{app}$ is higher during dry cycles and lower during wet cycles; this difference reduces with the progress of cycles.

In the following discussion, it shall be attempted to have another look at the mechanism of freeze-thaw damage in light of the observations above.

### 5.1.2 Drying Shrinkage

It was noticed that $\alpha_{app}$ increases when a concrete specimen is cooled below 0°C. Since concrete is known to shrink upon drying, it is proposed here that the increase in $\alpha_{app}$ is related to the wetting and drying of gel pores in concrete during the freeze-thaw process.

It is known that drying shrinkage is the result of removal of water from pores in concrete, creating a meniscus inside the pore and causing shrinkage due to surface tension of the residual water. This effect is not as well marked in the larger pores as it is in the smaller gel pores. If some process involves water being drawn out of the gel pores in concrete, it would lead to shrinkage of concrete and would also generate imbalance within the concrete pores. This imbalance would cause water to migrate back into the gel pores once the process that caused it to migrate out of the pores is reversed. This migration would cause concrete to swell back due to the refilling of the gel pores. This will be referred to as Wetting Expansion.

### 5.1.3 Initial Cycles

In the following discussion, references of 'larger' and 'smaller' pores pertain to the capillary pores in concrete and of 'gel' pores to the much finer inter-layer spacing containing strongly bonded water. Upon the start of the freeze-thaw cycles, the larger pores generally have lower saturations, while the gel pores have higher saturations (Fig. 5.1(a)). Water has been found to migrate to freezing sites in the larger pores from the gel pores during freezing. This process is called ice-accretion and is due to free energy gradient between unfrozen water in gel pores and ice in the larger pores (Fig. 5.1(b)). This process would cause drying of the gel pores and

lead to shrinkage of concrete as discussed above. The freezing sites, i.e. the larger pores, however, have a low saturation at this stage, and the expansion of water upon freezing is accommodated in the unfilled space. This process starts at temperatures below 0°C starting with the larger pores, and would continue till all the smaller pores are frozen at temperatures of around -25°C. This process is thus progressive in nature and will cause continuous drying of gel pores in the vicinity of the freezing sites with reduction in temperature till all pores are frozen.

This process would thus cause shrinkage, additional to the contraction that would be caused only by a change of temperature in the absence of this drying process. Since this process would occur only below 0°C, the observed cooling contraction would be higher below 0°C when compared to above 0°C and thus $\alpha_{app}$ will be higher during freezing below 0°C.

The opposite would happen upon thawing of pore water. During thawing, as the water in the pores begins to melt, an imbalance is generated. Since the energy of water increases upon thawing, an energy gradient no longer exists between the gel pores and the larger pores. However, a hydraulic difference is generated due to the higher saturation of larger pores compared to the gel pores. This hydraulic pressure would be stabilized by water flowing back into the gel pores (Fig. 5.1(c)). This process would again cause refilling of gel pores and hence lead to dilatation of concrete. This process would also continue in the range of temperatures where ice in the pores of different sizes would melt starting from the smaller pores till the water in the largest pores in concrete melts. The concrete would thus expand faster due to the wetting of the gel pores when compared to the expansion only due to temperature change in the absence of this wetting process. Again, since the process would occur only during thawing and under 0°C, $\alpha_{app}$ during thawing will be observed to be higher below 0°C than above 0°C.

### 5.1.4 Progressive Wetting of Specimens

When concrete has excess water present on its surface, the pore saturation would be higher closer to the surface when compared to away from the surface. This

saturation gradient can exist in equilibrium inside concrete due to the relatively low permeability of concrete and thus the high friction of flow. In the initial cycles, this saturation will not be high enough to generate overall expansions due to expansion of water in the pores. However, during thawing, as water migrates back to gel pores and the volume reduces due to melting of ice; a low pressure would be generated in the larger pores. Since at this time, the smaller pores closer to the surface would have already melted and would have a relatively higher saturation, water from these smaller pores would be sucked into the larger inner pores due to the pressure difference (Fig. 5.1(c)). Larger pores towards the center would thus continue to draw water from the smaller pores outside and water would thus progressively move towards the center. If any water is present on the surface of the specimen, it would be frozen at temperatures below 0°C. However, due to the partial emptying of the pores as described above, upon melting, water would enter the specimen from outside, increasing the overall water saturation of the concrete (Fig. 5.1(d)).

An increase in saturation of the pores would lead to further adsorption of water into the gel pores causing wetting expansions and thus increasing residual strains.

### 5.1.5 Dry Specimens

In cases where no water is available on the surface of the specimen, an inverse saturation gradient would exist within the concrete with higher saturations in the inner pores, than the outer pores. Thus, during thawing, water would progressively move from the inner smaller pores to the larger pores outside due to the low pressure generated by migration of water back to gel pores and reduction in volume upon melting of ice. So, in a process opposite to that discussed above when excess water is present on the concrete surface, water would progressively move out of the concrete surface due to the low humidity outside and lead to an overall reduction in saturation of the concrete, causing drying and thus reduction in residual strains. However, after the initial loss of water from the specimens, an equilibrium saturation gradient would be reached preventing further loss of water

into the surroundings. This would lead to a stabilization of residual strains in dry specimens after an initial reduction.

Reduced pore-saturation of concrete would lead to emptier pores and ice-accretion would be less restricted by pore volume. Higher migration of water from the gel pores to the larger pores, would thus be possible, causing higher drying during freezing. This would thus lead to higher drying shrinkage compared to cases of higher saturation and thus a higher $\alpha_{app}$ would be observed during freezing in dry cycles, compared to wet cycles.

Due to the higher degree of emptying of gel pores during freezing, the migration of water back to the gel pores during thawing would increase, again causing greater expansions during thawing compared to specimens with higher pore saturations, $\alpha_{app}$ would thus be higher during dry cycles when compared to wet cycles also during thawing.

Also, in the current test regime, even though the time period of the cycles for the dry specimens is the same as that in the wet specimens, the temperature range is smaller due to the low thermal diffusivity of air compared to water. If water is present around specimens, heat would be more effectively transferred from the temperature controls outside. The cooling rate is thus effectively lower in the dry specimens when compared to the wet specimens. This would also lead to higher degrees of drying of the gel pores as will be discussed in the next section.

With contributions of all the above described factors, comparatively higher values of $\alpha_{app}$ would thus be observed during dry cycles.

### 5.1.6 Slow Temperature Rate

The process of flow of water from the gel pores to the larger pores would be slow in nature owing to the small size and convoluted nature of the involved connections. In rapid freeze-thaw cycles, time plays an important role in preventing complete emptying of gel pores during freezing with all the water from

the gel pores unable to move to the freezing sites before the thawing starts. In slower cycles, however, higher amounts of water can diffuse out of the gel pores during freezing and can also diffuse back during thawing, since longer time periods are available for this migration. This growth in the drying and wetting of gel pores increases the additional drying related shrinkage during freezing and wetting related dilatation during thawing, in slow cycles when compared to the rapid cycles. $\alpha_{app}$ would thus be higher for slower temperature rates.

### 5.1.7 Progress of Deterioration

As water progressively moves into the specimens with the progress of the freeze-thaw cycles, saturation in the pores increases (Fig. 5.1(e)). The higher saturation of pores would prevent migration of water from the gel pores to the freezing sites due to the reduced free space available in the larger pores (Fig. 5.1(f)). Shrinkage of concrete due to movement of water out of the gel pores and thereafter back into the gel pores would thus be reduced as the saturation of the pores increases. This would result in an overall reduction in the observed $\alpha_{app}$ when compared to cases of lower pore saturations, thus leading to a continuous reduction in the value with the progress of deterioration due to the above described progressive ingress of water into the specimen.

Once the larger pores begin to saturate further, tensile forces would be generated within the pores due to expansion of water within the pores upon freezing. There would be expansion during freezing and contraction during thawing in the pores with higher saturations, thus reducing $\alpha_{app}$ further as deterioration progresses. This tensile pressure within the pores would also cause cracking in the vicinity of the saturated pores and increase the permeability of concrete (Fig. 5.1(g)). These newly generated cracks would be filled with water quicker owing to the higher permeability of the concrete thus increasing the overall water content in the specimen and also the deterioration rate (Fig. 5.1(h)-(j)). This increased deterioration rate, being in the form of expanding cracks, would thus be reflected in the measured residual strains.

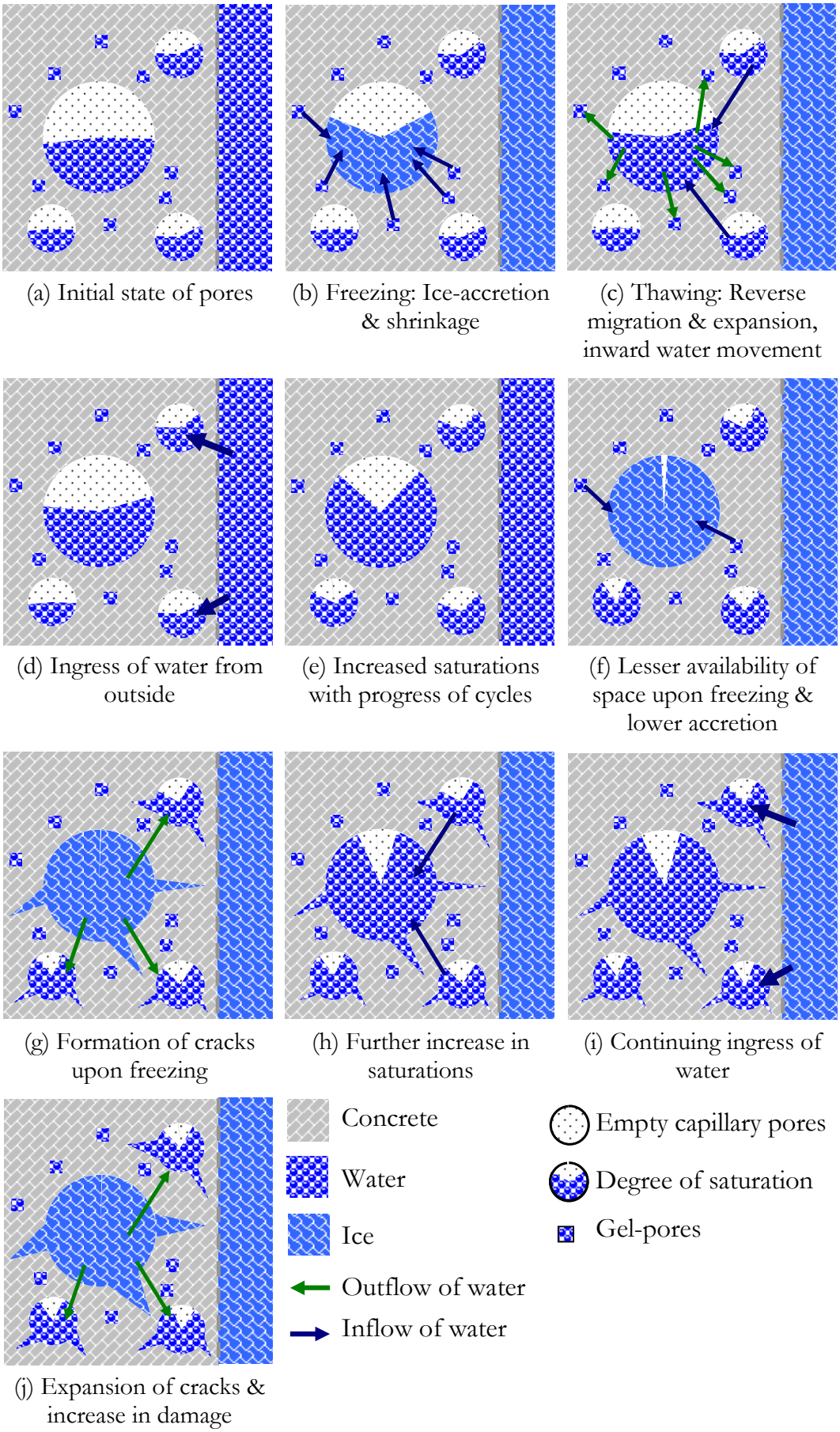


Fig. 5.1: The progress of freeze-thaw deterioration

### 5.1.8 Possible Reduction of $\alpha_{app}$ to a Constant Value

As discussed above, with the saturation of pores, propagation of cracks in the vicinity of saturated pores would lead to increasing residual strains. Since in the current discussion, $\alpha_{app}$ has been measured only for temperatures below -4˚C, expansion of concrete due to freezing of water in larger cracks will not be reflected in this value. $\alpha_{app}$ would thus be mainly affected by drying of gel pores and material contraction of concrete. In cases of high saturation, expansion of larger cracks and ingress of water into the specimen can thus continue without causing any further change in the movement of water from gel pores, thus allowing $\alpha_{app}$ to stay constant. Thus, at high saturations, if dilatation is limited to temperatures close to 0˚C, $\alpha_{app}$ can cease to reduce even as deterioration would continue with the growth of larger cracks.

### 5.1.9 Differences during Freezing and Thawing

In the above discussion, the observed increase in $\alpha_{app}$ during freezing has mainly been attributed to the drying of gel pores. So, theoretically, if the amount of water going back into the gel pores during thawing is more than that diffused out of it, $\alpha_{app}$ would be higher during thawing when compared to freezing part of a sub-zero freeze-thaw cycle.

As discussed above, the saturation of pores increases during the freeze-thaw cycles and upon melting, pores can withdraw water from proximate smaller pores towards the surface having a relatively higher saturation. This would lead to a higher saturation of the pores upon melting than before freezing, not considering the water gained from the gel pores. Higher saturation levels in nearby larger pores would thus lead to an increased migration of water into the gel pores during thawing when compared to the amount of water that migrated out during freezing.

In cases of higher saturation, $\alpha_{app}$ may be even higher during thawing when compared to thawing. Expansion of water in highly saturated pores would lead to generation of new cracks in concrete and also to the growth of newer cracks. This would thus lead to expansion in concrete during freezing, reducing the $\alpha_{app}$

observed during freezing. A large part of these expansions being irreversible due to non-closing water-filled cracks, the contraction upon thawing of ice would be lesser than the expansion observed during freezing. $\alpha_{app}$ would thus be observed to be much smaller during freezing than during thawing in highly saturated specimens with high deterioration rates.

This has been noticed only during the slower cycles in the current experiments since due to hysteresis and high thermal gradients within the specimens during the rapid cycles, it was difficult to calculate $\alpha_{app}$ for freezing and thawing individually in the sub-zero region.

### 5.1.10 Effect of Size of Specimen

It has been noticed that, in case of smaller specimens, $\alpha_{app}$ was observed to be higher and residual strains lower. Smaller specimens allow easier and faster redistribution of pore-water when compared to the larger specimens. A larger surface area to volume ratio would enable higher water losses from the specimen during freezing thus reducing the cracking of the specimens and allowing higher movement of water from gel pore to the freezing sites in the empty space generated by the movement of water out of the specimen. Owing to the higher ice-accretion possible in the smaller specimens, $\alpha_{app}$ would be observed to be higher when compared to the larger specimens. The residual strains would also be lower since lower pore saturations would lead to lesser crack growths and hence smaller expansions.

Very large specimens, however, would be expected to show an inverse behavior. Time required for saturating the innermost pores of larger specimens being higher, the damage in very large specimens would be restricted to outer regions and would progress inwards. Also, the temperature ranges would be lower for the inner parts of the specimen, thus subjecting it to less severe conditions. An optimal specimen size should thus exist for which the highest residual strains should be observed for similar surface conditions.

### 5.1.11 Effect of Air-Entrainment

A well air-entrained concrete would have a well distributed air-void system throughout its volume with an optimal void spacing that allows for movement of water into the voids upon the application of pressures that would otherwise cause damage to the concrete, without compromising the strength of the concrete itself by increasing the void content (Fig. 5.2(a)). The movement of water from gel-pores to freezing sites generates pressures within the system that can be reduced if some of this migrating water can be temporarily accommodated in voids without saturating them and applying excessive pressures on its walls. Air voids can thus reduce the pressure in proximate pores and allow for higher migration of water from gel pores to the freezing sites without excessively increasing pressures (Fig. 5.2(b)). However, upon thawing, and reduction of pressures in the pore, the air pressure inside the air-void would force the water out of the void and back into the larger pores and the gel pores (Fig. 5.2(c)). This would cause higher drying and wetting during freezing and thawing respectively and thus lead to a higher $\alpha_{app}$ when compared to a non-air-entrained specimen. Also, the expulsion of water from the air-voids upon thawing would increase the pressure in the pore, preventing the ingress of water as discussed above in §5.1.4 (Fig. 5.2(d)).

When air-entrained specimens are subjected to alternate wetting and drying along with cyclic freezing and thawing, the initial dry cycles would lead to a loss of excess water from the surface of the specimens and the behavior would be somewhat similar to that of a non-air-entrained specimen described above. However, with the progress of freeze-thaw cycles, equilibrium would be reached where the water entering the concrete during the wet cycles would not affect the rate of ice-accretion since it would be accommodated in the air-voids upon freezing. The water being shed during the dry cycles would also be reduced since a large amount of water that would have instead moved out of the specimen would be accommodated in air voids. Also, the small amount of water still shed during the dry cycles, would still not lead to increased ice-accretion since most of the water being shed from the concrete would have been accommodated in air-voids during freezing and would not have hindered ice-accretion. A stable value of $\alpha_{app}$

would thus be reached when the air-voids would act as buffer for the water being absorbed during wet cycles and shed during the dry cycles.

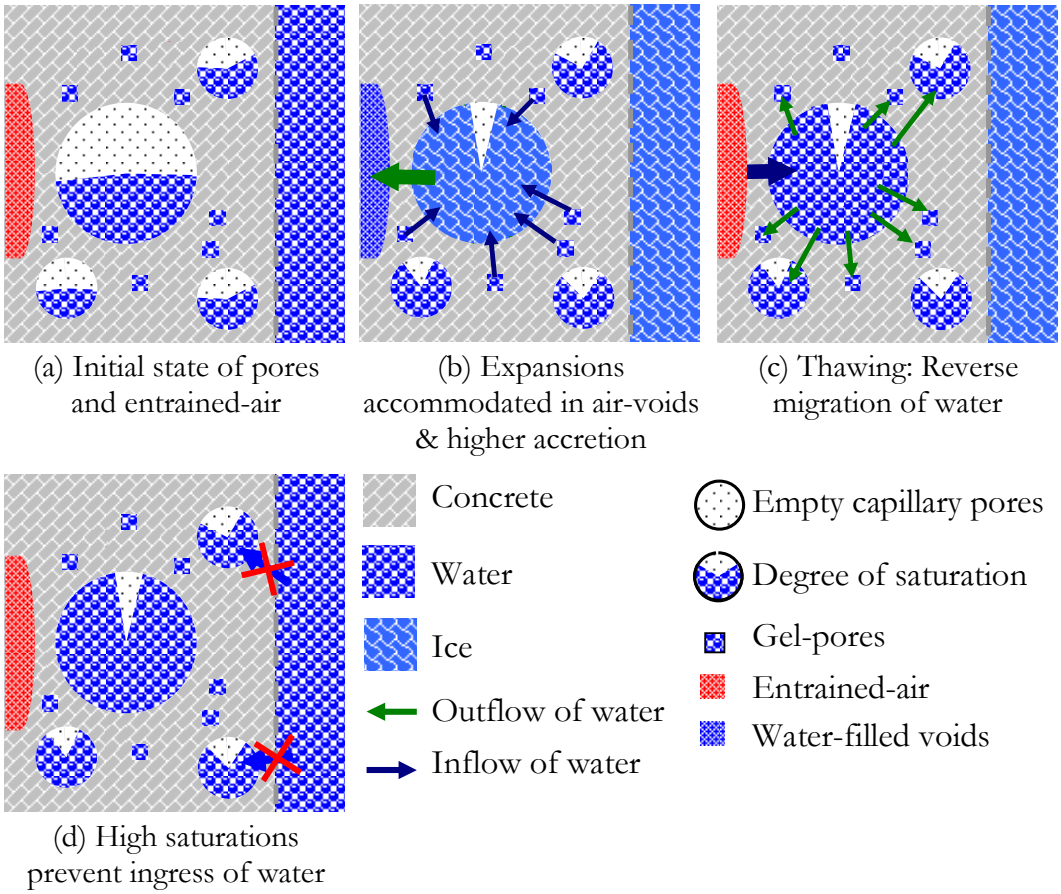


Fig. 5.2: Effect of air-entrainment

Thus lower tensile forces leading to lesser cracks and lesser irreversible drying and wetting of air-entrained specimens would also reduce the residual strains in air-entrained specimens. Air-entrainment would thus be an effective measure against freeze-thaw deterioration provided the air-voids are properly distributed, as has already been shown by many researchers (See §2.2, §2.3.2).

## 5. 2 PROCESS OF FREEZE-THAW DETERIORATION

Based on the above discussion, the process during cyclic freezing and thawing can be summarized as below:

- Freezing causes movement of water from gel pores to larger pores, thus drying them and increasing the contraction in concrete during freezing, due to the low initial saturation of the larger pores.

- Upon thawing, water migrates back to gel pores increasing the expansion of concrete upon thawing.
- The movement of water to and from gel pores is a slow process and is higher for slow temperature rates.
- Reduction in volume upon thawing causes water to move progressively from outer pores to inner pores and into the concrete if available outside.
- Progressive movement of water into the concrete increases residual strains due to wetting expansion.
- Increased saturation of pores prevents water from gel pores to enter the larger pores and reduces the extent of drying during freezing, and hence wetting of the gel pores during thawing, also reducing the apparent thermal expansion coefficient of concrete.
- Upon reaching threshold saturation levels, expansion of water generates tension, leading to cracks and increasing both, the permeability of concrete and the free space available for water.
- Upon thawing, cracks cannot close completely due to presence of water resulting in increasing residual strains.
- With an increased permeability, the rate of water ingress increases, leading to increased deterioration rates.
- Entrained air buffers volume changes in water upon phase change and prevents further ingress of water and growth of cracks, thus arresting damage in concrete.

## 5.3 SUBSTANTIATIONS OF PROGRESSIVE INGRESS

### 5.3.1 Dilatations around 0˚C

Overall dilatations upon freezing have been observed between 0˚C and -5˚C in specimens with high deteriorations. This shows the presence of large saturated cracks within the specimens. Freezing in large size cracks would occur at temperatures close to 0˚C and the expansion of water in these cracks would cause expansion of concrete. Since this dilatation was not observed in the initial cycles, it

can be concluded that with the progress of freeze-thaw cycles, a large amount of water migrates into the specimen, as explained in the previous section as the basis of variation of $\alpha_{app}$ with deterioration.

### 5.3.2 Severe Growth of Cracks in Pre-Cracked Specimens

The observations from experimental Series 5, in which pre-cracked reinforced-concrete specimens were subjected to cyclic freezing and thawing, have been discussed in §3.3.3. In this series, severe growth of cracks was observed in un-entrained specimens submerged under water, while the deterioration in air-entrained specimens and specimens in dry state was much smaller. Also, as shown in Table 3.9 earlier, the smaller specimens were able to withstand comparatively more number of cycles. In order to consider these observations in light of the above discussion, the cracked specimen can be considered to behave similar to a specimen with severe freeze-thaw damage.

According to the above discussion, in the presence of water around the specimens, cyclic freezing and thawing would induce water to grow in the region around the cracks due to high permeability of concrete around the cracks. However, this would not be the case for regions away from the cracks. The dilatations in concrete would thus start to occur much earlier than the rest of the specimen generating high pressures in the region near the cracks since it would restrained by the relatively unsaturated stronger concrete away from the cracks and the reinforcement bar. This process would result in large localized stresses near the cracks causing severe localized damage. This damage would cause loss of concrete from the vicinity of the cracks and hence increase the crack width. The increase in crack width would further increase the permeability and increase the rate of damage. So, according to the discussion above, the cracked specimens would have very severe and rapid localized deterioration, as was observed in Series 5.

The presence of continuous water ingress leading to a growth in cracks can also be realized by a comparison between specimens discussed above, in which ingress of water was allowed by the presence of excess water around the specimens, and

the specimens where such ingress was not allowed by keeping the surface of the specimen in a dry state. Since little crack growth was observed in specimens under dry conditions, ingress of water from outside, and not the action of water already present inside concrete can be attributed as the main cause of damage in the other specimens. It must be reminded here that the specimens were continuously submerged under water for long periods before testing and thus had reasonably high saturations at the start of testing.

Similar to the un-entrained specimens, air-entrained specimens would also be highly saturated in the regions around the cracks. However, a proper distribution of air voids through the concrete volume would accommodate most of the expansion of water even in the regions of high saturation. This water would be expelled from the voids upon thawing, allowing for accommodation of water expansion during successive cycles. Localized stresses around the cracks in air-entrained specimens would thus be low and hence it would be expected that air-entrainment would restrict crack growth. Further, the expulsion of water from air-voids back to the pores would prevent further ingress of water through the crack due to little space available within the pores. Air-entrainment would thus restrict both, dilatation of concrete due to expansion of water, and further ingress of water, thus preventing growth of a pre-induced crack in an air-entrained specimen, as was observed in the experiments under discussion.

The above discussion, once again substantiates the occurrence of progressive water-ingress into concrete and its role as a major cause of freeze-thaw deterioration. Also, the effectiveness of air-entrainment in preventing water from entering concrete can once again be perceived.

# Chapter 6

# MONITORING FREEZE-THAW DETERIORATION AND VULNERABILITY

The importance of studying strain variations in concrete during cyclic freezing and thawing has been highlighted in the earlier discussion. From the above discussion, it can be explicitly seen that monitoring of strains in concrete can help achieve great insight into the process of freeze-thaw deterioration and can help us better monitor deterioration. The biggest strength of use of strains in measuring deterioration lies in the ability to obtain continuous measurements of strain even from remote locations. Three main aspects of strain variations: strain-temperature trends, residual strains, and apparent thermal expansion coefficients have been discussed in this study. How these three aspects would play an important role in monitoring the health and vulnerability of concrete to freeze-thaw action has been discussed in the following sections.

## 6.1 STRAIN-TEMPERATURE TREND

It can be derived from earlier discussion that strain-temperature trend of 'healthy' concrete would display no discontinuous behavior and dilatations upon freezing. Dilatations in concrete at specific temperatures would show the presence and growth of cracks within the concrete and thus the vulnerability of concrete. It was seen that it is possible to closely predict strain variations in concrete for specific thermal gradients, thus providing base expected values around which observed values should lie. Large deviations from the expected values can indicate deterioration.

However, it is important to be able to identify faulty readings either due to malfunctioning hardware or localized effects around the strain-gauges. From the above discussed experiments, it has been noticed that the strain-temperature behavior of concrete is generally smooth in nature with no sharp peaks observed. Sharp peaks were, however, observed in case of local effects around strain gauges. In such cases care has to be taken to neglect data around intermittent sharp effects. Also, continuous scatter in data would indicate hardware fault leading to unreliable data throughout the range of observed temperatures.

## 6.2 RESIDUAL STRAINS

Residual strains can be used as a quantitative measure of freeze-thaw deterioration. From the above study, it was observed that residual strains, when measured at the same temperature, depend on two main factors: level of deterioration, and degree of saturation. The following discussion considers the main observations regarding the use of residual strains for measuring deterioration.

### 6.2.1 Uniform Moisture Conditions

Residual strains can provide the most accurate measurements of deterioration in cases where the monitored specimen is continuously under same external moisture condition. In such cases, residual strains are seen to rise monotonously with increasing deteriorations. It has been observed that residual strains can also be used to measure small and slow deteriorations which might otherwise go undetected using conventional methods.

### 6.2.2 Degree of Saturation

Residual strains are found to increase with an increasing degree of saturation of concrete. It was also observed that the degree of pore saturation increases due to cyclic freezing and thawing. This increase in saturation would lead to an increase in residual strains. Though, this increase does not signify deterioration, however, it does signify the vulnerability of the concrete to deteriorate, since higher pore saturations would cause higher freeze-thaw vulnerabilities. It is thus important to

measure individual effects of increase in saturation and deterioration to study the damage and vulnerability of concrete.

### 6.2.3 Freezing Expansions

A large part of expansions during freezing cannot be measured once the water inside concrete thaws due to closing of cracks upon reduction of volume of water upon thawing. Residual strains should thus be measured at temperatures below 0°C so as to also reflect reversible freezing expansions. However, sudden changes around 0°C can cause a large scatter in the observed data and reduce accuracy. Use of data around 0°C should thus be avoided in such measurements. Such sudden changes should however be monitored separately for anomalies as discussed in §4.1.2.

### 6.2.4 Varying External Conditions

Strains are found to reduce upon drying of concrete and increase upon wetting. The reduction in strain upon drying is partly due to drying shrinkage of concrete as discussed in Chapter 5. Drying of concrete can also lead to closing of cracks that were formed earlier further reducing residual strains. Such reductions in strain, however, would not signify an improvement in concrete condition. However, they can reduce the vulnerability of concrete and the rate of further damage. It is thus important to monitor moisture conditions around and within the specimen to be able to identify contributions of wetting and drying and to calculate the increase in residual strain solely due to deterioration.

## 6.3 APPARENT THERMAL EXPANSION COEFFICIENT

The variation of apparent thermal expansion coefficient ($\alpha_{app}$) due to freeze-thaw deterioration has been discussed at length in Chapter 5. It was observed that the value of $\alpha_{app}$ below 0°C remains high in cases of low deterioration and reduces in cases of high deterioration. Also, reductions in $\alpha_{app}$ are accompanied by further increase in deterioration rates. $\alpha_{app}$ can thus be used effectively to monitor the vulnerability of concrete to freeze-thaw deterioration. Reductions in values of $\alpha_{app}$

would signify an increase in concrete saturation and thus a higher risk of damage during further freeze-thaw cycles. In cases of observed reduction of the value, measures to reduce concrete saturation would have to be taken in order to prevent deterioration.

In the current study, $\alpha_{app}$ was measured only from data below -4°C in order to avoid errors due to crack expansions and slower temperature rates near 0°C due to freezing of water around the specimens. Similar precautions would have to be taken in order to avoid possible errors according to the exposure conditions. Though expansions close to freezing would also reduce $\alpha_{app}$ signifying high damages, it is suggested that they be considered separately. This would allow studying both crack growth and formation of new cracks due to increasing saturation of pores.

## 6.4 SUGGESTED FURTHER RESEARCH

Though the treatment of strain-measurements for deterioration monitoring in this study is not absolute, its potential use has been studied and the main factors affecting its use as a monitoring method have been identified. A much wider experimental study on larger specimens would be required to be able to quantitatively interpret the monitored strains in terms of structural health and vulnerability. Specific topics considered important for furthering this research have been listed below.

- Variation of strains in actual structures under cyclic freezing and thawing
- Variation of strains at different locations in a large specimen subjected to cyclic freezing and thawing
- Variations of strains in concrete with saturation degree at different temperatures
- Calculation of variation of saturation degree at different locations inside a specimen for given environmental variations
- Correlation between residual strains and conventional testing methods

# Chapter 7

# CONCLUSIONS

In the current study an interesting variation of strains in concrete both with temperature and deterioration was observed. It has been shown that though the temperature-strain behavior of concrete is close to linear elastic in the initial stages, with the increase of deterioration diversion from the ideal behavior increases. Experiments on various specimens showed that freeze-thaw deterioration generates residual strains in concrete, which if measured, can provide a reliable estimate of the level of deterioration. However, various other factors such as the saturation degree also have to be accounted for proper interpretation of results.

It was found that presence of excess water around specimens can increase the severity of deterioration by several degrees of magnitude. A closer look at the obtained results showed a progressive ingress of water into concrete as being the main reason of deterioration in specimens submerged under water. Almost no damage was observed in similar specimens kept in dry conditions.

Air-entrainment was found to effectively prevent progressive ingress of water thus preventing deterioration. Air-entrainment was found to be effective even in extreme conditions such as in the vicinity of flexural cracks.

Measurements of various parameters in strain-temperature variations shows cyclic wetting and drying of gel pores taking place along with cyclic freezing and thawing. This process was found to reduce strains in concrete during thawing to different degrees depending on the vulnerability and deterioration of concrete. A study of variations of this wetting and drying of gel pores gives us a better understanding

of processes during cyclic freeze-thaw deterioration. It was also seen that continuous measurement of variation of apparent thermal expansion coefficient, which directly depends on wetting and drying of gel pores and freezing expansions of pore water, can be used to monitor the progress of deterioration in concrete by providing crucial information regarding saturation levels of concrete pores.

It was thus seen in this study that measurement of macroscopic strain can give a better understanding of the complex microscopic processes taking place during cyclic freezing and thawing and can be potentially used for quantitative evaluation of deterioration in concrete due to exposure to cyclic freezing and thawing.

# REFERENCES


1. Attiogbe, E.K., "Mean spacing of air voids in hardened concrete", ACI Materials Journal, Vol. 90, No. 2, 1993, pp. 174-181
2. Bouzoubaâ, N., Lachemi, M., Miao, B., and Aïtchin, P.-C., "Thermal damage of mass concrete: experimental and numerical studies on the effect of external temperature variations", Canadian Journal of Civil Engineering, National Research Council, Canada, Vol. 24, No. 4., 1997, pp. 649-657
3. Defay, R., Prigogine, I., Bellemans, A., and D.H. Everett, "Surface Tension and Adsorption", Wiley, New York, 1966
4. Detwiler, R.J., Dalgleish, B.J., and Williamson, R.B., "Assessing the durability of concrete in freezing and thawing", Vol. 86, No. 1, 1989, pp. 29-35
5. Fagerlund, G, "The critical degree of saturation method of assessing the freeze/thaw resistance of concrete", Materiaux et constructions, Vol. 10, No. 58, 1977, pp. 217-229
6. Hasan, M., Okuyama, H., Sato, Y., and Ueda, T., "Stress-strain model of concrete damaged by freezing and thawing cycles", Journal of Advanced Concrete Technology, Japan Concrete Institute, Vol. 2, No. 1, 2004, pp. 89-99
7. Hulshizer, A.J., "Air-entrainment control or consequences", Concrete International, American Concrete Institute, Vol. 19. No. 7, 1997, pp. 38-40
8. Jacobsen, S., Marchand, J., and Hornain, H., "SEM observations of the microstructure of frost deteriorated and self-healed concretes", Cement and Concrete Research, Vol. 25, No. 8, 1995, pp. 1781-1790
9. Kaneuji, M., Winslow, D.N., and Dolch, W.L., "The relationship between an aggregate's pore size distribution and its freeze thaw durability in concrete", Cement and Concrete Research, Vol. 10, No. 3, 1980, pp. 433-441
10. Kleiner, V.D., "An evaluation of frost action on concrete", Concrete International, American Concrete Institute, Vol. 18, No. 3, 1996, pp.42-43
11. Lide, D.R., Ed., "Handbook of chemistry and physics", Chemical Rubber Company, 81st edition, 2000
12. Litvan, G., and Sereda, P.J., "Particulate admixture for enhanced freeze-thaw resistance of concrete", Cement and Concrete Research, Vol. 8, No. 1, 1978, pp. 53-60
13. Litvan, G., "Further study of particulate admixtures for enhanced freeze-thaw resistance of concrete", Journal of the American Concrete Institute, Vol. 82, No. 5, 1985, pp. 724-730
14. Macinnis, C., and Lau, E.C., "Maximum aggregate size effect on frost resistance of concrete", Vol. 68, No. 2, 1971, pp. 144-149

15. MacInnis, C., and Whiting, J.D., "The frost resistance of concrete subjected to a deicing agent", Cement and Concrete Research, Vol. 9., No. 3., 1979, pp. 325-335
16. Maekawa, K., and Okamura, H., "The deformational behavior and constitutive equation of concrete using the elasto-plastic and fracture model", Journal of the Faculty of Engineering, the University of Tokyo, Vol. XXXVII, No. 2, 1983, pp. 253-328
17. Maekawa, K., Chaube, R., and Kishi, T., "Modelling of concrete performance; Hydration, microstructure formation and mass transport", E. & F.N. Spon, 1999
18. Marchand, J., Pleau, R. and Gange, R., "Deterioration of concrete due to freezing and thawing", Materials Science of Concrete IV, American Ceramic Society, 1995, pp. 283-354
19. Mehta, P.K., and Monteiro, P.J.M., "Concrete microstructure, properties, and materials", First Indian Edition, Indian Concrete Institute, 1997
20. Miura, T., and Lee, D.H., "Deformation and deterioration of concrete subjected to cyclic cooling down to very low temperatures", Proceedings of the National Research Council, Canada, Second Canada/Japan Workshop on Low Temperature Effects on Concrete, 1991, pp. 23-37
21. Ohta, T., "Freeze-thaw durability of concrete structures in Hokkaido", Proceedings of the National Research Council, Canada, Second Canada/Japan Workshop on Low Temperature Effects on Concrete, 1991, pp. 161-190
22. Penttala, V., "Freezing-induced strains and pressures in wet porous materials and especially in concrete mortars", Advanced cement based matter, Vol. 7, No. 1, 1998, pp. 8-19
23. Penttala, V., and Al-Neshawy, F., "Stress and strain state of concrete during freezing and thawing cycles", Cement and Concrete research, Vol. 32, No. 9, 2002, pp. 1407-1420
24. Philleo, R.E., "A method for analyzing void distribution in air-entrained concrete", Cement, concrete and aggregates, Vol. 5, 1983, pp. 128-130
25. Pigeon, M., Prevost, J., and Simard, J.M., "Freeze-Thaw durability versus freezing rate", Journal of the American Concrete Institute, Vol. 82, No. 5, 1985, pp. 684-692
26. Pigeon, M., Gagne, R., Aitchin, P.C., and Banthia, N, "Freezing and thawing tests of high-strength concretes", Cement and Concrete Research, Vol. 21, No. 5, 1991, pp. 844-852
27. Pigeon, M., and Pleau, R., "Durability of concrete in cold climates", E. & F.N. Spon, 1995
28. Pleau, R., and Pigeon, M., "The Use of the Flow Length Concept to Assess the Efficiency of Air Entrainment with Regards to Frost Durability: Part I—Description of the Test Method", Cement, concrete and aggregates, Vol. 18. No. 1, 1996, pp. 19-29

29. Pigeon, M., Talbot, C., Marchand, J. and Hornain, H., "Surface microstructure and scaling resistance of concrete", Cement and Concrete Research, Vol. 26, No. 10, 1996, pp. 1555-1566
30. Powers, T.C., "A Working Hypothesis for Further Studies of Frost Resistance of Concrete", Journal of American Concrete Institute, Vol. 16, No. 4, 1945, pp. 245-272
31. Powers, T.C., "The air requirements of frost-resistant concrete", Proceedings of the highway research board, Portland cement association, Bulletin 33, 1949, pp. 1-28
32. Powers, T.C., and Helmuth, R.A., "Theory of volume changes in hardened Portland-cement paste during freezing", Proceedings of Highway Research Board, Vol. 32, 1953, pp. 285-297
33. Powers, T.C., "Void Space as a Basis for Producing Air-Entrained Concrete", Journal of the American Concrete Institute, Vol. 25, No. 9, 1954, pp. 741-760
34. Schulson, E.M., "Ice Damage to Concrete", Cold Regions Research and Engineering Laboratory Special Report, US Army Corps of Engineers, No. 98-6, 1998
35. Snyder, K.A., "A Numerical Test of Air Void Spacing Equations", Advanced Cement Based Materials, Vol. 8, No. 1, 1998, pp. 28-44
36. Taber, S., "Frost heaving." Journal of Geology, Vol. 37, 1929, pp.428-461
37. Zuber, B., and Marchand, J., "Modeling the deterioration of hydrated cement systems exposed to frost action: Part 1: Description of the mathematical model", Cement and Concrete Research, Vol. 30, No. 12, 2000, pp. 1929-1939